Supporting Information

Construction of polymethine chain modified pentamethylene cyanine dyes for G-quadruplex imaging in live cells

Li Guan*[a], Jun Li[a], Yanyan Zhou[a], Anyang Li[c], Lili Yin*[b], Wenhui Guan[a], and Yile Fu*[a]

[a] School of Chemistry and Chemical Engineering, Xi'an University of Architecture and Technology, Xi'an, 710055, P. R. China
[b] International Medical Department, The Second Hospital of Dalian Medical University, No. 467 Zhongshan Road, Shahekou District, Dalian, 116027, P. R. China
[c] Key Laboratory of Synthetic and Natural Functional Molecule of the Ministry of Education, National Demonstration Center for Experimental Chemistry Education, College of Chemistry and Materials Science, Northwest University, Xi'an 710127, P. R. China

Table of contents

Ⅰ Experimental Section

1. Materials and Regants

All reagents and solvents used in this study were purchased from commercial sources. Dimethyl sulfoxide (DMSO), Methanol (MeOH), Ethyl acetate (EA), Petroleum benzin (PE), 1,4-dioxane, Dichloromethane (DCM) and Ethanol (EtOH) were purchased from Tianjin FuYu Fine Chemical Co. Ltd. (China). Glycerol was purchased from Shanghai Macklin Biochemical Co. Ltd. (China), Tris-HCl Solution (1M, pH=7.4) and PBS buffer was purchased from Shanghai Sangon Biotech Co. Ltd (China). Potassium iodide (KI) was purchased from Qingdao Tocean Iodine Products Co. Ltd (China). Potassium carbonate (K_2CO_3) was purchased from Gu'anxian Jingqiu Chemical Industry Co. Ltd (China). DNase I and RNase A were purchased from Shanghai Sangon Biotech Co. Ltd. (China). Mitochondrial membrane potential assay kit with JC-1, Golgi Green, Hoechst 33342, Lyso-Tracker Green and Mito-Tracker Green was purchased from Beyotime Biotechnology (China). All oligonucleotides used in this work were synthesized and purified by Shanghai Sangon Biotechnology Co., Ltd (China), and the sequences are listed in Table S1.

2. Preparation of oligonucleotides

All lyophilized oligonucleotides were dissolved in 10 mM Tris−HCl buffer solution (pH 7.4, containing 60 mM KCl) for DNA stock solutions (100 μM). The stock solutions of the oligonucleotides c-myc, c-kit2, htg22, and oxy28 were annealed at 95°C for 10 min, cooled naturally to room temperature to form G4, and then stored for more than 24 h at 4°C before using. Duplex DNA (108D and ds26) and single stranded DNA (da21 and dt21) stock solutions were prepared by heating the self-complementary strand at 85°C for 5 min in the Tris−HCl buffer, followed by slow cooling over 6 h.

Table S1. Oligonucleotide sequences used in this work.

DNA	Sequence (5` to 3`)	Structure	Biological origin
c-myc	TGAGGGTGGGTAGGGTGGGTAA	parallel G4	promoter
c-kit2	CGGGCGGGCGCGAGGGAGGGT	parallel G4	promoter
oxy28	GGGTTTTGGGGTTTTGGGGTTTTGGGG	antiparallel G4	telomere
htg22	AGGGTTAGGGTTAGGGTTAGGG	hybrid G4	telomere
108D	CGCTAGCG	duplex	-
ds26	CAATCGGATCGAATTCGATCCGATTG	duplex	-
da21	AAAAAAAAAAAAAAAAAAAA	single stranded	-
dt21	TTTTTTTTTTTTTTTTTTTT	single stranded	-

3. Instrumentations

HRMS analysis was done using a QTOF mass spectrometer and NMR spectra were detected by Bruker Neo 600 M. ^{1}H NMR titration spectra were detected by AVANCE III HD 700MHz (Bruker). Absorption and emission spectra for all the compounds were performed with a Purkinje General TU-1900 UV/Vis spectrometer (China) and a F-320 fluorescence spectrophotometer (Tianjin Gangdong Sci. &Tech. Co. Ltd, China), respectively. Circular dichroism spectra were characterized by a Chirascan circular dichroism spectrophotometer. The cells imaging was performed on andor live cell confocal imaging platform (Nikon Instruments Inc.), using Olympus FV1000 MPE with a microscope IX 71, a 100×/NA 1.40 oil objective lens.

4. Synthesis of cyanine dyes

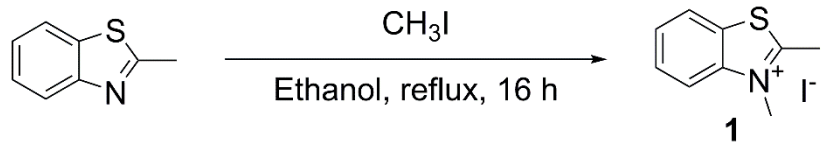

1

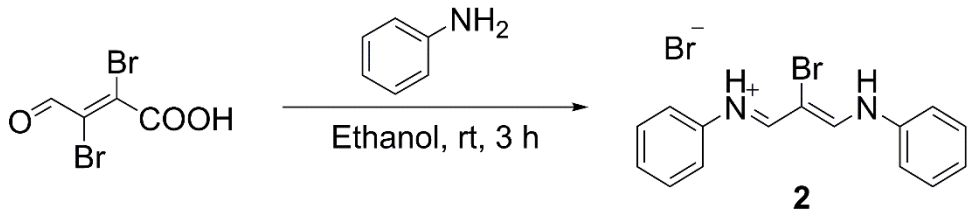

2

Compounds **1**[1] and **2**[2] have been synthesized according to literature known procedures.

Synthesis of 2,3-dimethylbenzo[d]thiazol-3-ium iodide (1). 2-methylbenzothiazole (2.00 g, 13.40 mmol) in anhydrous ethanol (10 mL) and iodomethane (5.71 g, 40.20 mmol, 3.0 eq) were stirred and refluxed for 16 h. Upon cooling to room temperature, the precipitate was filtered, washed with cold ethanol and dried under vacuum to afford the product **1** as a white solid (2.95 g, 77%). HRMS (ESI-TOF) m/z: $[M-I]^+$ calcd for $C_9H_{10}NS^+$ 164.0528, found 164.0579.

Synthesis of N-((1E,2Z)-2-Bromo-3-(phenylamino)allylidene)benzenaminium Bromide (2). Into a 100 mL of 3-necked round-bottom flash was added aniline (0.80 g, 8.59 mmol, 2.2 eq) in EtOH (10 mL), and a solution of dibromo-4-oxobut-2-enoic acid (1.00 g, 3.91 mmol, 1.0 eq) in EtOH was added dropwise at room temperature under N_2 atmosphere. The resulting mixture was stirred for 3 h at room temperature. After cooling to 0°C with ice-water bath, the precipitated solid was collected by filtration and washed with Et_2O (15 mL). This resulted in the desired product **2** as a yellow solid (1.03 g, 70%). HRMS (ESI-TOF) m/z: $[M-HBr+Na]^+$ calcd for $C_{15}H_{13}BrN_2Na^+$ 323.0160, found 323.0217; This product was directly used in the next reaction without further purification.

All compounds were synthesized by borrowing from our previous method with slight modifications. The synthesized route is shown in the Scheme S1.

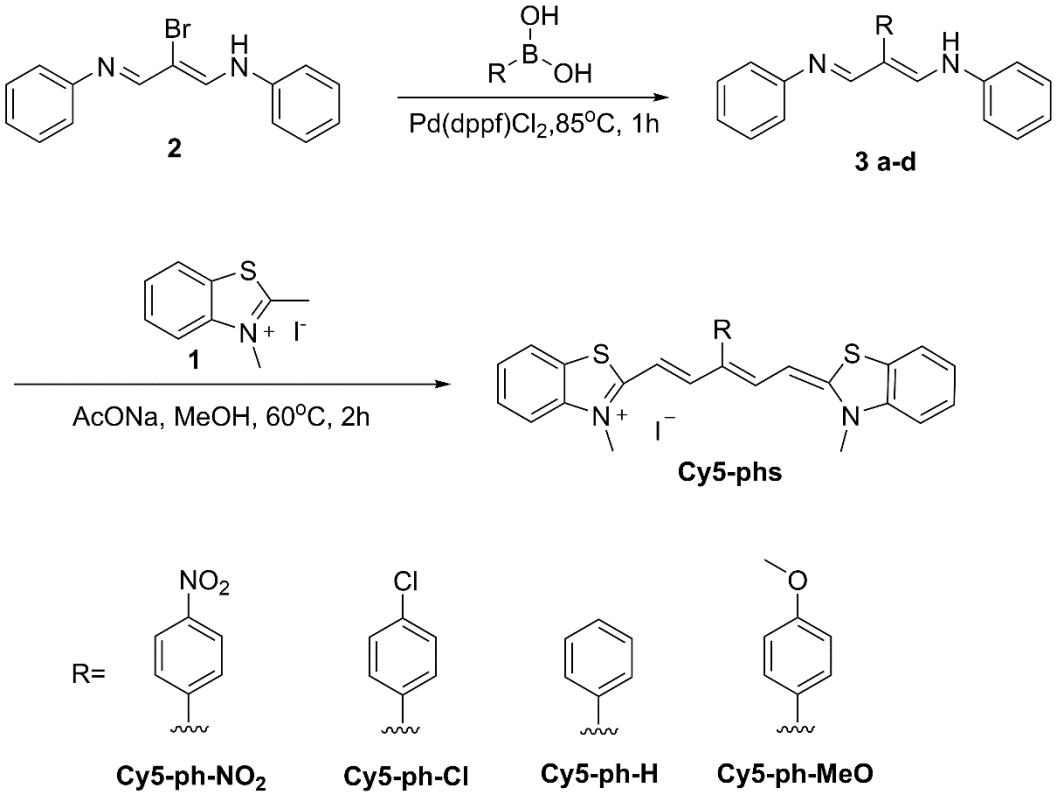

Scheme S1. Schematic of the synthesis of **Cy5-phs** derivatives.

Synthesis of 3a. Compound **2** (380 mg, 1 mmol, 1.0 eq), 4-nitrophenylboronic acid (183 mg, 1.1 mmol, 1.1 eq.), $Pd(dppf)Cl_2$ (35 mg, 0.05 mmol, 0.05 eq), and K_2CO_3 (415 mg, 3 mmol, 3.0 eq) were dissolved in 12 mL 1,4-dioxane/H_2O (v/v 5/1) and stirred at 85°C for 1 h under N_2 atmosphere. Finally, the solvents were evaporated and the residue was purified by column chromatography (silica gel; eluent: n-hexane/AcOEt = 10/1) to give **3a** as yellow solid (189 mg, 56%). HRMS (ESI-TOF) m/z: $[M+H]^+$ calcd for $C_{21}H_{18}N_3O_2^+$ 344.1477, found 344.1447.

Synthesis of Cy5-ph-NO_2. Compound **3a** (59 mg, 0.17 mmol, 1.0 eq), compound **1** (105 mg, 0.36 mmol, 2.1 eq), and anhydrous NaOAc (56 mg, 0.68 mmol, 4.0 eq) were dissolved in methanol (2 mL) and stirred by heating at 60°C for 2 h under N_2 atmosphere. The progress of the reaction was monitored by TLC (MeOH/CH_2Cl_2 1/10, R_f=0.22). Upon cooling, the mixture was added dropwise into aqueous KI solution and stirred for 10 min. and finally filtered to obtain the crude product. The crude product was collected by filtration and purified by column chromatography (silica gel; eluent: MeOH/CH_2Cl_2 = 1/100) to afford **Cy5-ph-NO_2** as dark green solid (52 mg,

50%). ^{1}H NMR (600 MHz, DMSO-*d*6) δ 8.41 (d, *J* = 8.5 Hz, 2H), 8.06 (d, *J* = 7.9 Hz, 2H), 8.01 (d, *J* = 13.8 Hz, 2H), 7.73 (d, *J* = 8.3 Hz, 2H), 7.66 (d, *J* = 8.5 Hz, 2H), 7.58 (t, *J* = 7.6 Hz, 2H), 7.44 (t, *J* = 7.6 Hz, 2H), 5.93 (d, *J* = 13.8 Hz, 2H), 3.67 (s, 6H). ^{13}C NMR (151 MHz, DMSO-*d*6) δ 165.77, 149.94, 147.09, 143.96, 142.43, 131.79, 128.53, 127.51, 125.77, 125.68, 124.91, 123.52, 114.17, 98.28, 34.08. HRMS (ESI-TOF) m/z: $[M-I]^+$ calcd for $C_{27}H_{22}N_3O_2S_2^+$ 484.1148, found 484.1152.

Synthesis of 3b. Compound **2** (380 mg, 1 mmol, 1.0 eq), 4-chlorophenylboronic acid (171 mg, 1.1 mmol, 1.1 eq.), Pd(dppf)Cl_2 (35 mg, 0.05 mmol, 0.05 eq), and K_2CO_3 (415 mg, 3 mmol, 3.0 eq) were dissolved in 12 mL 1,4-dioxane/H_2O (v/v 5/1) and stirred at 85°C for 1 h under N_2 atmosphere. Finally, the solvents were evaporated and the residue was purified by column chromatography (silica gel; eluent: n-hexane/AcOEt = 10/1) to give **3b** as yellow solid (107 mg, 32%). HRMS (ESI-TOF) m/z: $[M+H]^+$ calcd for $C_{21}H_{18}ClN_2^+$ 333.1253, found 333.1138.

Synthesis of Cy5-ph-Cl. Compound **3b** (57 mg, 0.17 mmol, 1.0 eq), compound **1** (105 mg, 0.36 mmol, 2.1 eq), and anhydrous NaOAc (56 mg, 0.68 mmol, 4.0 eq) were dissolved in methanol (2 mL) and stirred by heating at 60°C for 2 h under N_2 atmosphere. The progress of the reaction was monitored by TLC (MeOH/CH_2Cl_2 1/10, R_f=0.19). Upon cooling, the mixture was added dropwise into aqueous KI solution and stirred for 10 min. and finally filtered to obtain the crude product. The crude product was collected by filtration and purified by column chromatography (silica gel; eluent: MeOH/CH_2Cl_2 = 1/100) to afford **Cy5-ph-Cl** as dark green solid (43 mg, 54%). ^{1}H NMR (600 MHz, DMSO-d_6) δ 8.03 (d, *J* = 7.9 Hz, 2H), 7.94 (d, *J* = 13.6 Hz, 2H), 7.69 (d, *J* = 8.3 Hz, 2H), 7.63 – 7.53 (m, 4H), 7.43 – 7.34 (m, 4H), 5.85 (d, *J* = 13.6 Hz, 2H), 3.63 (s, 6H). ^{13}C NMR (151 MHz, DMSO-d_6) δ 165.37, 142.49, 132.81, 132.21, 129.84, 128.55, 125.69, 123.55, 114.10, 98.35, 34.01.HRMS (ESI-TOF) m/z: $[M-I]^+$ calcd for $C_{27}H_{22}ClN_2S_2^+$ 473.0907, found 473.0885.

Synthesis of 3c. Compound **2** (380 mg, 1 mmol, 1.0 eq), Phenylboronic acid (134 mg, 1.1 mmol, 1.1 eq.), Pd(dppf)Cl_2 (35 mg, 0.05 mmol, 0.05 eq), and K_2CO_3 (415 mg, 3 mmol, 3.0 eq) were dissolved in 12 mL 1,4-dioxane/H_2O (v/v 5/1) and stirred at 85°C for 1 h under N_2 atmosphere. Finally, the solvents were evaporated and the residue was purified by column chromatography (silica gel; eluent: n-hexane/AcOEt = 10/1) to give **3c** as yellow solid (113 mg, 38%). HRMS (ESI-TOF) m/z: $[M+H]^+$ calculated for $C_{21}H_{19}N_2^+$ 299.1407, found 299.1544.

Synthesis of Cy5-ph-H. Compound **3c** (51 mg, 0.17 mmol, 1.0 eq), compound **1** (105 mg, 0.36 mmol, 2.1 eq), and anhydrous NaOAc (56 mg, 0.68 mmol, 4.0 eq) were dissolved in methanol (2 mL) and stirred by heating at 60°C for 2 h under N_2 atmosphere. The progress of the reaction was monitored by TLC (MeOH/CH_2Cl_2 1/10, R_f=0.20). Upon cooling, the mixture was added dropwise into aqueous KI solution and stirred for 10 min. and finally filtered to obtain the crude product. The crude product was collected by filtration and purified by column chromatography (silica gel; eluent: MeOH/CH_2Cl_2 = 1/100) to afford **Cy5-ph-H** as dark green solid (37mg, 50%). ^{1}H NMR (600 MHz,) δ 7.97 (d, *J* = 7.6 Hz, 2H), 7.89 (d, *J* = 13.5 Hz, 2H), 7.63 (d, *J* = 8.1 Hz, 2H), 7.53 (t, *J* = 6.8 Hz, 2H), 7.49 (t, *J* = 7.5 Hz, 2H), 7.44 (t, *J* = 6.9 Hz, 1H), 7.35 (t, *J* = 7.3 Hz, 2H), 7.30 (d, *J* = 7.0 Hz, 2H), 5.79 (d, *J* = 13.4 Hz, 2H), 3.53 (s, 6H).^{13}C NMR (151 MHz, DMSO-d_6) δ 165.04, 150.50, 142.40, 130.15, 129.66, 128.45, 128.33, 126.85, 125.57, 123.46, 113.93, 98.43, 33.84. HRMS (ESI-TOF) m/z: $[M-I]^+$ calculated for $C_{27}H_{23}N_2S_2^+$ 439.1297, found 439.1279.

Synthesis of 3d. Compound 2 (380 mg, 1 mmol, 1.0 eq), 4-Methoxyphenylboronic acid (131.96mg, 1.1mmol, 1.1eq), Pd(dppf)Cl_2 (35 mg, 0.05 mmol, 0.05 eq), and K_2CO_3 (415 mg, 3 mmol, 3.0 eq) were dissolved in 12 mL 1,4-dioxane/H_2O (v/v 5/1) and stirred at 85°C for 1 h under N_2 atmosphere. The residue was purified by column chromatography (silica gel; eluent: *n*-hexane/AcOEt = 10/1) to afford **3d** as yellow solid (105 mg, 32%). HRMS (ESI-TOF) m/z: $[M+H]^+$ calculated for $C_{22}H_{21}N_2O^+$ 329.1575, found 329.1641.

Synthesis of Cy5-ph-MeO. Compound **3d** (56 mg, 0.17 mmol, 1.0 eq), compound **1** (105 mg, 0.36 mmol, 2.1 eq), and anhydrous NaOAc (56 mg, 0.68 mmol, 4.0 eq) were dissolved in methanol (2 mL) and stirred by heating at 60°C for 2 h under N_2 atmosphere. The reaction was monitored by TLC (MeOH/CH_2Cl_2 1/10, R_f=0.20). The crude product was purified by column chromatography (silica gel; MeOH/CH_2Cl_2 1/50) to afford **Cy5-ph-MeO** as dark green solid (46 mg, 58%). ^{1}H NMR (600 MHz, DMSO-d_6) δ 8.03–7.98 (m, 2H), 7.89 (d, *J* = 13.4 Hz, 2H), 7.66 (d, *J* = 8.3 Hz, 2H), 7.53 (dd, *J* = 8.5, 7.4, 1.3 Hz, 2H), 7.39 (t, *J* = 7.6 Hz, 2H), 7.30–7.24 (m, 2H), 7.15–7.10 (m, 2H), 5.87 (d, *J* = 13.5 Hz, 2H), 3.86 (s, 3H), 3.59 (s, 6H). ^{13}C NMR (151 MHz, DMSO-*d*6) δ 164.87, 159.03, 150.82, 142.40, 131.33, 128.42, 125.58, 125.51, 123.42, 115.01, 113.88, 98.51, 55.58, 33.85. HRMS (ESI-TOF) m/z: $[M-I]^+$ calculated for $C_{28}H_{25}N_2OS_2^+$ 469.1403, found 469.1380.

5. Experimental Methods

Stock solutions of dyes (10 mM) were prepared in dimethyl sulfoxide (DMSO).

UV/vis Spectroscopy. The absorption spectra were acquired using a Purkinje General TU-1900 UV-vis spectrometer at room temperature using a quartz cuvette with an optical path of 4 mm×10 mm. The concentration of dyes was diluted to 5 μM with MeOH, H_2O, Tris-HCl, PBS buffer, and 90% Glycerol, respectively. The absorbance of different dyes in different solvents was detected.

UV/vis Titration experiment. The concentration of dyes was diluted to 5 μM with 10 mM Tris−HCl buffer solution (pH 7.4, containing 60 mM KCl). Then gradually add different equivalent ratios of c-myc while detect the absorbance. A quartz cuvette with 4 mm×10 mm path length was used for the spectra recorded. The absorption spectra was collected from 400nm to 800nm.

Fluorescence Spectroscopy. The emission spectra were acquired using F-320 spectrometer at room temperature using a quartz cuvette with an optical path of 10 mm×10 mm. The concentration of dyes was diluted to 5 μM with MeOH, H_2O, Tris-HCl, PBS buffer and 90% Glycerol, respectively. The fluorescence intensity of different dyes in different solvents was detected.

Disaggregation experiment. The concentration of dyes was diluted to 5 μM with a mixed solution of different MeOH/Tris-HCl buffer rations (MeOH fraction is 0% ~ 90%). The UV/vis absorbance and fluorescence intensity were detected.

Fluorescence Titration experiment. The concentration of dyes was diluted to 5 μM with 10 mM Tris−HCl buffer solution (pH 7.4, containing 60 mM KCl) for fluorescence measurements. The fluorescence spectra were acquired using F-320 at room temperature. A quartz cuvette with 4 mm×10 mm path length was used for the spectra recorded at 10 nm and 10 nm for excitation and emission slit widths, respectively. The excitation wavelength was 588 nm and the fluorescence spectra were collected from 600 to 850 nm. The data from the fluorescence titrations were analysed by nonlinear fitting of independent site models according to the relevant literature. The association constant K_a was calculated from fluorescence titration data using the following equation:

$$\frac{F}{F_0} = 1 + \frac{Q-1}{2}\left[A + 1 + \sqrt{(A+1+x)^2 - 4x}\right]$$

where F_0 is the fluorescence intensity of dye (maximum emission wavelength) in the absence of DNA and F_{max} is the fluorescence intensity upon saturation of DNA. $Q = F_{max}/F_0$, $A = (K_aC_{dye})^{-1}$, and $x = nC_{DNA}\,(C_{dye})^{-1}$.

Calculation of fluorescent quantum yields. Spectroscopic measurements were carried out under the same conditions using rhodamine 800 (Φ=0.25, in ethyl alcohol)[3] as a standard and the relative fluorescence quantum yields of the dyes were calculated by the following equation:

$$\Phi_x = \Phi_s \frac{F_x A_S \lambda_{exs}}{F_S A_x \lambda_{exx}} \left(\frac{n_x}{n_s}\right)^2$$

where Φ represents the fluorescence quantum yield, F is the integrated area of the fluorescence spectrum, A is the absorbance at the excitation wavelength, λ_{ex} is the excitation wavelength, n is the refractive index of the solution (at low concentrations the refractive index of the solution is replaced by the refractive index of the solvent), and the x and s represent the sample to be measured and the reference standard respectively.

Light stability analysis. The concentration of dyes was diluted to 5 μM with deionized water. Under the lamp, the sample is taken every ten minutes to detect the absorbance of **Cy5-phs**.

Theoretical calculation. Density functional theory calculations, including the geometry optimization and molecular orbitals were performed by density functional theory (DFT) calculations at B3LYP/6-31+G (d, p) level. The optimized structures with minimum energies were confirmed by absence of imaginary frequencies. All the above calculations were performed by the Gaussian 16 program package[4]. Molecular orbitals are drawn by Multiwfn 3.8[5] and VMD 1.9.3 programs.

LOD calculation. Limit of detection (LOD) experiment was calculated by plotting the changes in the emission maximum as a function of G4s concentration. LOD was calculated according to the following equation:

$$LOD = \frac{S_b * k}{m}$$

where S_b is the standard deviation calculated out of 20 independent measurements on blank solution, k is 3, according to IUPAC recommendations and m is the slope obtained from the linear fitting.

G4 ligand competition experiment. The concentration of **Cy5-ph-H** was diluted to 5 μM with 10 mM Tris−HCl buffer solution (pH 7.4, containing 60 mM KCl), and add equal amount of c-myc

($n_{c\text{-}myc}/c_{dye}$=1:1). Then gradually add TMPyP4, and detect the change of fluorescence intensity of 5μM **Cy5-ph-H-**c-myc complex with the stepwise addition of TMPyP4 in 10mM Tris-HCl buffer, 60mM KCl, pH 7.4.

Continuous variation analysis. Working solution of **Cy5-ph-H** (5 μM) and G4s (5 μM) were prepared in 10 mM Tris−HCl buffer solution (pH 7.4, containing 60 mM KCl). Fluorescence spectra were recorded for solutions with varying mole fractions of **Cy5-ph-H** and G4 DNA using a quartz cuvette with 2 mm×10 mm path length (the sum of **Cy5-ph-H** and G4 DNA concentrations was kept constant at 5 μM). Then fluorescence values at λ_{em} wavelength corresponding to the molar fraction of ligand were plotted to generate a Job plot.

Circular dichroism spectroscopy. The CD spectra were recorded on a Chirascan circular dichroism spectrophotometer in the wavelength range 220−320 nm using a 4 mm quartz cuvette at room temperature. The scanning speed of the instrument was set to 200 nm/s. G4 DNA was diluted to a 5 μM working solution with 10 mM Tris−HCl buffer solution (60 mM KCl, pH 7.4) and the dye **Cy5-ph-H** was added over a range of 0-4 mol equivalents. The CD spectra were recorded after equilibrating for 10 min. The CD melting assay was performed at a fixed concentration of G4s (5 μM) in 10 mM Tris-HCl buffer (60 mM KCl, pH 7.4). The data were recorded at intervals of 2.5℃ over a range of 25-90°C, with a heating rate of 1.0°C/min. CD melting profile was measured at 265 nm for parallel G4 and 295 nm for hybrid/antiparallel G4s.

Molecular docking. The docking study of parallel G4 c-myc (PDB ID: 2L7V) and dsDNA 108D (PDB ID: 108D) with **Cy5-ph-H** was performed using AutoDock 4.2.6 program and Lamarck genetic algorithm. The σ bonds between atoms in the **Cy5-ph-H** molecule were all set as rotatable bonds, and the DNA was regarded as a rigid structure for semi-flexible docking. During the docking process, a 120×120×120 step docking square box was set on the DNA binding site, and **Cy5-ph-H** was docked 200 times independently at the binding site. The binding conformation with the lowest docking energy was selected to determine the binding field and binding mode of DNA and **Cy5-ph-H**, and the docking results were analyzed and viewed with Open-Source PyMOL (version 2.3.0) software.

NMR Studies. G4 samples were prepared in potassium phosphate buffer (25 mM KH_2PO_4, 10% D_2O, 100 mM KCl, pH 7.4) The final concentration of G4 was 300 μM, titrated with increasing amounts of **Cy5-ph-H**. Experiments were performed on a 700MHz spectrometer at 25℃.

Interference resistance test. The concentration of dyes was diluted to 5 μM with 10 mM

Tris−HCl buffer solution (pH 7.4, containing 60 mM KCl). Then add different species (1:blank; 2: c-myc; 3: Ba^{2+}; 4: Ca^{2+}; 5: Cd^{2+}; 6: Cu^{2+}; 7: Fe^{3+}; 8: K^{+}; 9: Mg^{2+}; 10: Na^{+}; 11:Ni^{+}; 12:Pd^{2+}; 13: Cr^{3+}; 14: CO_3^{2-}; 15: NO_3^{-}; 16: SO_4^{2-}; 17 H_2O_2; 18: GSH; 19: Cys), and detected the fluorescence intensity.

Cell cytotoxicity. Cells (HepG2, WT) were seeded into 96-well plates and incubated for 24 h to achieve complete attachment (approximately 2×10^4 cells per well). Then 0.1 μM, 1 μM, 5 μM of DMSO dye solution (set as three replicates for each concentration) and incubated for 24 h with the same dose of DMSO (0.1%) in the control group. After incubation, CCK-8 solution（10 μL/well）was added to the 96-well plates and subsequently incubated at 37°C incubator for 2 h. Then the absorbance at 450 nm was measured using a microplate reader (Thermo Multiskan GO) and relative cell survival rate (%) was calculated. Cytotoxicity experiments were performed in three technical replicates.

Cell Culture and Imaging. All the cells were cultured in Dulbecco's modified Eagle's medium (Gibco, Grand Island, NY, USA) with 10% (v/v) fetal bovine serum (Gibco) and 1% (v/v) penicillin sodium and streptomycin (Gibco) at 37°C with 5% CO_2, and allowed to adhere for 24 h before use. Live and fixed cells imaging: After HepG2 cells were washed three times with PBS, they were fixed with 4% paraformaldehyde for 15 min. Fixed and live cells were incubated with 0.5 μM **Cy5-ph-H** (0.1% DMSO) at 37°C for 10 min. After removal of the working buffer, PBS was added and the cells were imaged on a laser confocal scanning microscope. Time-lapse imaging of live HepG2 cells: After live HepG2 cells were washed three times with PBS, the culture dish was fixed on the objective stage of a laser confocal scanning microscope to select the appropriate field of view through the white field. Then the probe (0.5 μM, 0.1% DMSO) was added quickly, and the acquisition of images proceeded synchronously. Settings were beat every 5 s for a total shot duration of 10 min. For the co-localization study, cells were first treated with 0.5 μM **Cy5-ph-H** (0.1% DMSO) at 37°C for 20 min, then incubated with Hoechst 33342 (2 μg/mL) for 10 min; Golgi green (5 μM) for 30min at 4℃, then added BSA solution to cells and incubated for 1 h at room temperature after washed for three times; Lyso-Tracker Green (0.075 μM) for 45 min; Mito-Tracker Green (0.2 μM) for 40 min, respectively. After removal of the working buffer, PBS was added and the cells were imaged on a laser confocal scanning microscope. The excitation wavelengths were 405 nm for Hoechst 33342, 488 nm for Golgi green, Lyso-Tracker Green and

Mito-tracker Green, 640 nm for **Cy5-ph-H**, respectively. The cell imaging fluorescence intensity generated on the cell was analyzed and quantified using the ImageJ software.

Mitochondrial membrane potential experiment. Confocal fluorescence microscope images of HepG2 cells incubated with 10 μM CCCP (Carbonyl cyanide 3-chlorophenylhydrazone) for 1h and then incubated with JC-1 staining working solution (Mitochondrial membrane potential assay kit with JC-1, C2006, Beyotime Biotechnology) or 0.5 μM **Cy5-ph-H** for 20 min, respectively. The cells were imaged on a laser confocal scanning microscope. The excitation wavelengths were 488 nm for JC-1 monomer, 561 nm for JC-1 aggregation, and 640 nm for **Cy5-ph-H**, respectively.

Intracellular G4 ligand TMPyP4 competitive binding experiment. HepG2 cells were washed with PBS buffer, then incubated with 0.5 μM **Cy5-ph-H** at 37°C for 20 minutes, followed by three washes with PBS. Next, they were incubated with TMPyP4 at various concentrations (0 μM, 10μM, 20μM) for 1h, washed three times with PBS, and then imaged on a laser confocal scanning microscope. The cell imaging fluorescence intensity generated on the cell was analyzed and quantified using the ImageJ software.

DNase or RNase Digestion Tests. HepG2 cells were fixed with 4% paraformaldehyde for 15 min and then processed with 0.1% Triton-X 100/PBS at 37°C for 30 min. The fixed cells were first incubated with 100 units mL^{-1} RNase-free DNase I and RNase A at 37°C for 10 h, with the addition of PBS as control. After that, the cells were stained with 2 $\mu g \cdot mL^{-1}$ DAPI and 0.5 μM **Cy5-ph-H** (0.1% DMSO) for 10 min each. The cells were imaged on a laser confocal scanning microscope. The cell imaging fluorescence intensity generated on the cell was analyzed and quantified using the ImageJ software.

Ⅱ Supplementary Figures

Table S2. Crystallographic data of **Cy5-ph-H**

Crystal data	**Cy5-ph-H**
CCDC number	2218822
Empirical formula	$C_{54}H_{52}I_2N_4O_3S_4$
Formula weight	1187.04
Temperature	150(2) K
Wavelength	0.71073
Crystal system	Triclinic
Space group	P -1
Unit cell dimensions volume	a=10.702(2) α=107.310(6) b=11.213(2) β=104.509(6) c=12.216(2) γ =102.423(6)
Z	1
Calculated density	1.532 Mg/m^3
Absorption coefficient	1.431 mm^{-1}
F(000)	598
Crystal size	0.33 x 0.25 x 0.18 mm
Theta range for data collection	2.00 to 27.70 deg.
Limiting indices	-14<=h<=13, -14<=k<=14, -15<=l<=15
Reflections collected/unique	37943 / 5923 [R(int) = 0.1515]
Completeness to theta = 27.70	98.5%
Absorption correction	Semi-empirical from equivalents
Max. and min. transmission	0.773 and 0.657
Refinement method	Full-matrix least-squares on F^2
Data/restraints/parameters	5923 / 0 / 309
Goodness-of -fit on F^2	1.090
Final R indices [I>2sigma(I)]	R1 = 0.0989, wR2 = 0.2256
R indices (all data)	R1 = 0.1668, wR2 = 0.2558
Largest diff. peak and hole	1.924 and -1.967 $e.A^{-3}$

Optical spectroscopy

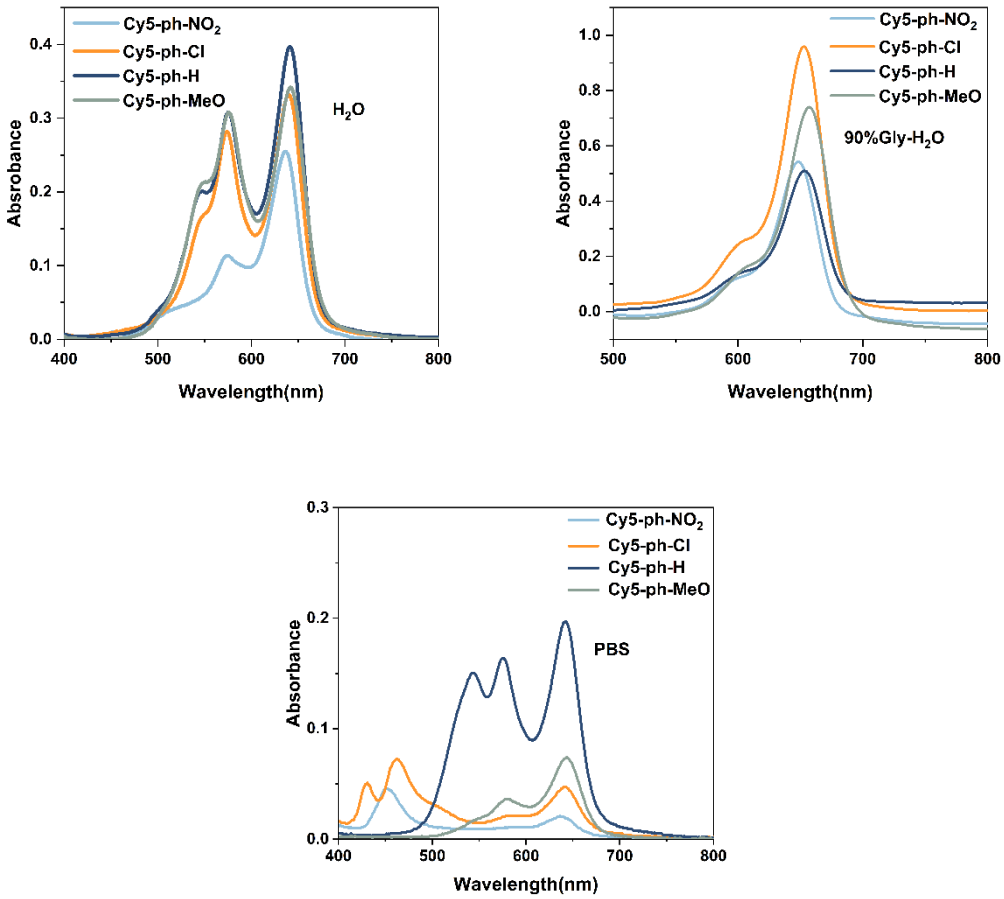

Fig. S1. UV/vis absorption spectra of 5 μM **Cy5-phs** in different solvents.

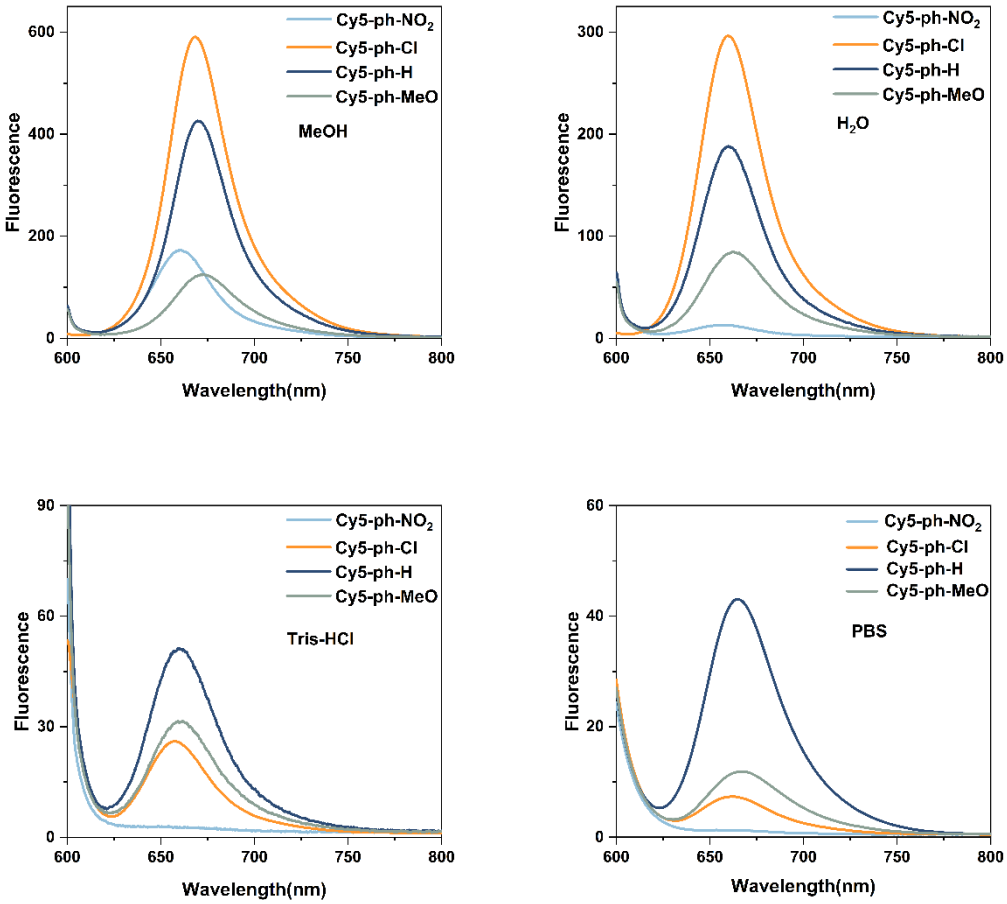

Fig. S2. Fluorescence spectra of 5 μM **Cy5-phs** in different solvents.

Table S3. Summary of spectroscopic properties of **Cy5-phs** in different solvents.

	Solvent	**λ_{abs} (nm)**	**$\varepsilon \times 10^5$ ($M^{-1}cm^{-1}$)**	**λ_{em} (nm)**	**Stokes shift (nm)**	**Φ**
Cy5-ph-NO_2	MeOH	640	1.22	660	20	0.049
	H_2O	637	0.51	655	18	0.008
	Tris-HCl	633	0.011	-	-	0.052
	PBS	636	0.042	-	-	0.011
	90% glycerol-H_2O	649	1.08	667	18	-
Cy5-ph-Cl	MeOH	644	2.09	668	24	0.11
	H_2O	640	0.66	660	20	0.072
	Tris-HCl	641	0.03	657	16	0.091
	PBS	640	0.09	661	21	0.021
	90% glycerol-H_2O	653	1.92	674	28	-
Cy5-ph-H	MeOH	646	2.72	670	24	0.066
	H_2O	641	0.79	660	19	0.038
	Tris-HCl	641	0.10	659	18	0.10
	PBS	642	0.39	664	22	0.019
	90% glycerol-H_2O	654	1.02	672	18	-
Cy5-ph-MeO	MeOH	648	1.80	672	24	0.03
	H_2O	642	0.68	662	20	0.018
	Tris-HCl	642	0.16	660	18	0.025
	PBS	644	0.15	665	21	0.021
	90% glycerol-H_2O	657	1.48	680	23	-

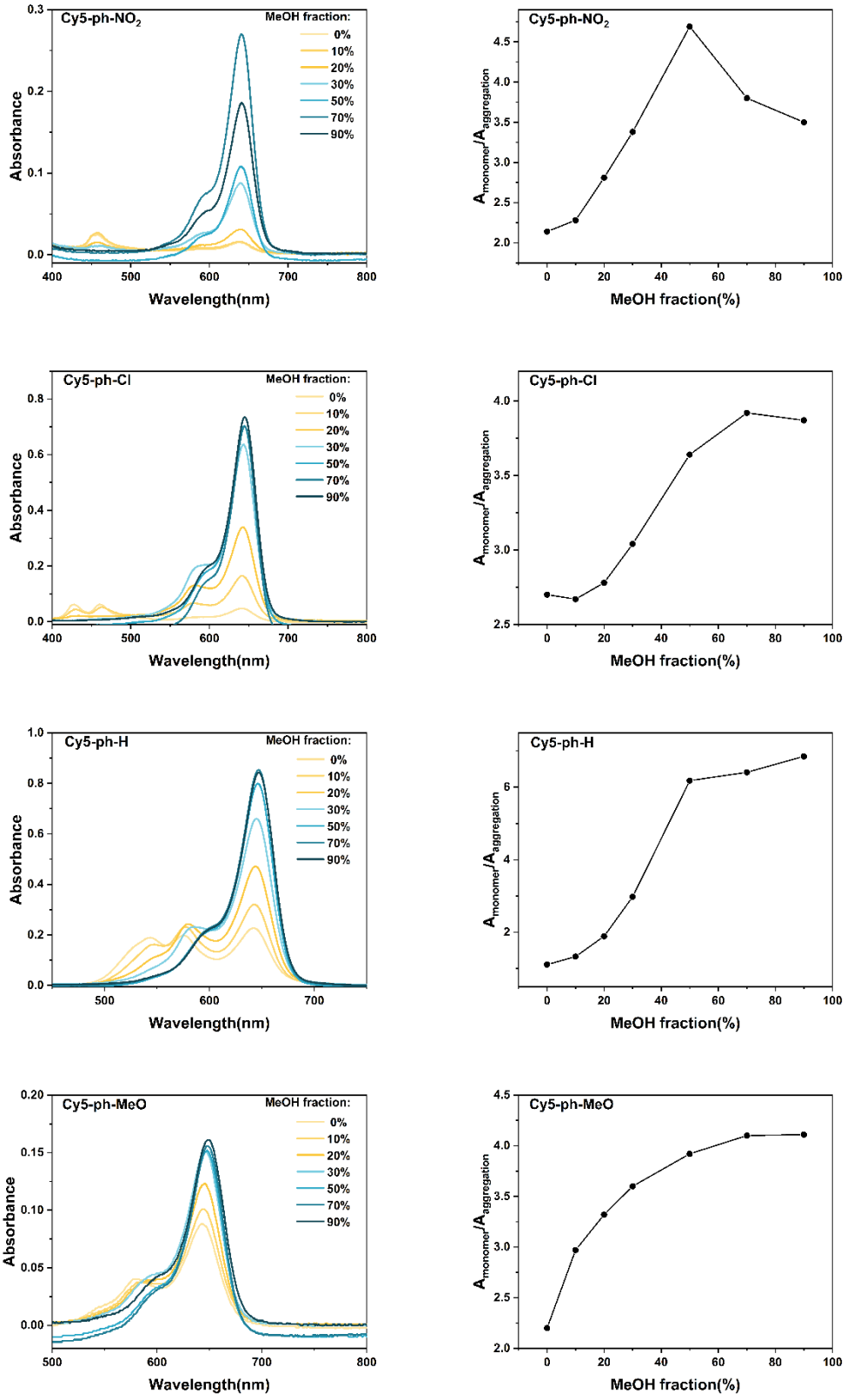

Figure S3. UV/vis absorption spectra of 5 μM **Cy5-phs** in different ratios of MeOH/Tris-HCl buffer (60 mM K^+) systems.

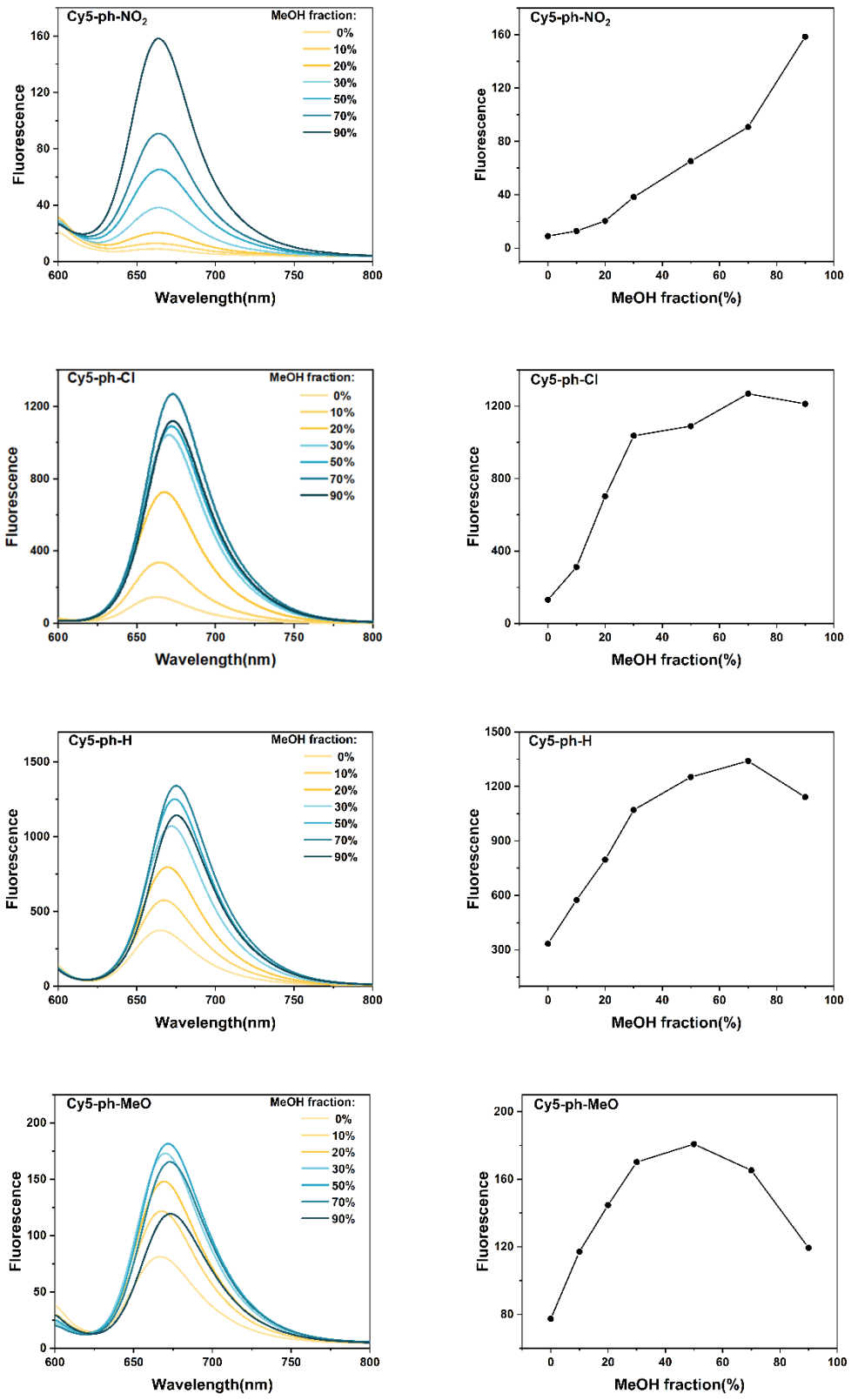

Figure S4. Fluorescence spectra of 5 μM **Cy5-phs** in different ratios of MeOH/Tris-HCl buffer (60 mM K^+) systems.

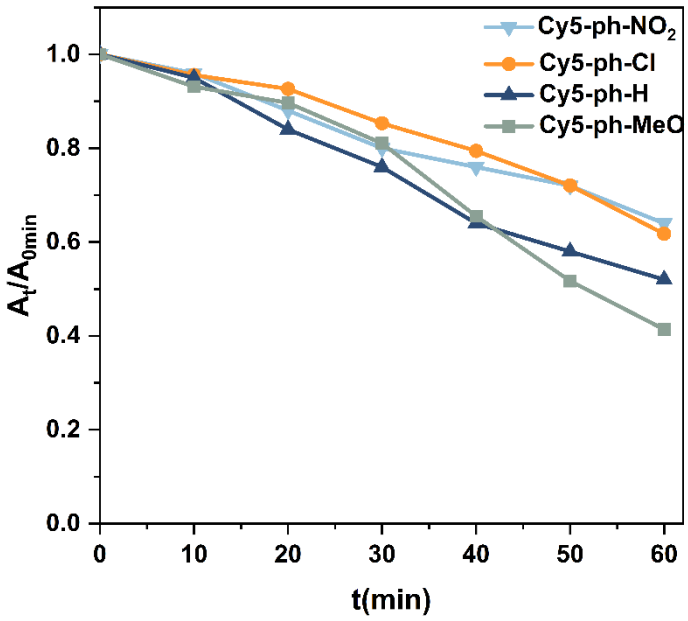

Fig. S5. Photostability of 5 μM **Cy5-phs.**

Theoretical calculation

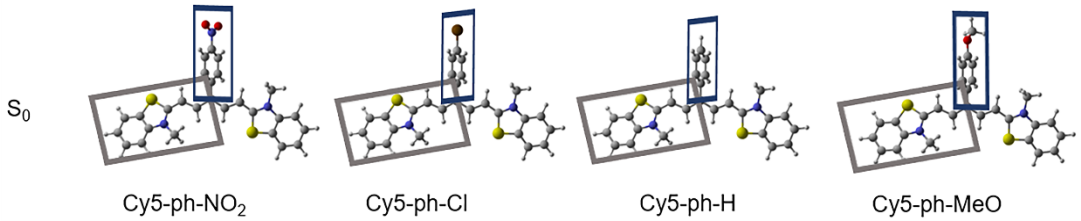

Fig. S6. The molecular structure torsion of the ground state.

Table S4. The result of theoretical calculation

Dye	Orbits	Excitation energy (eV)	λ_{abs} (nm)	Oscillator strength
Cy5-ph-NO$_2$	HOMO -> LUMO (S_0-S_1)	1.6621	745.95	0.0894
	HOMO -> LUMO+1 (S_0-S_2)	2.2934	540.61	1.9966
Cy5-ph-Cl	HOMO->LUMO (S_0-S_1)	2.2826	543.17	2.0461
Cy5-ph-H	HOMO->LUMO (S_0-S_1)	2.2781	544.25	2.0484
Cy5-ph-MeO	HOMO->LUMO (S_0-S_1)	2.2605	548.48	1.9828

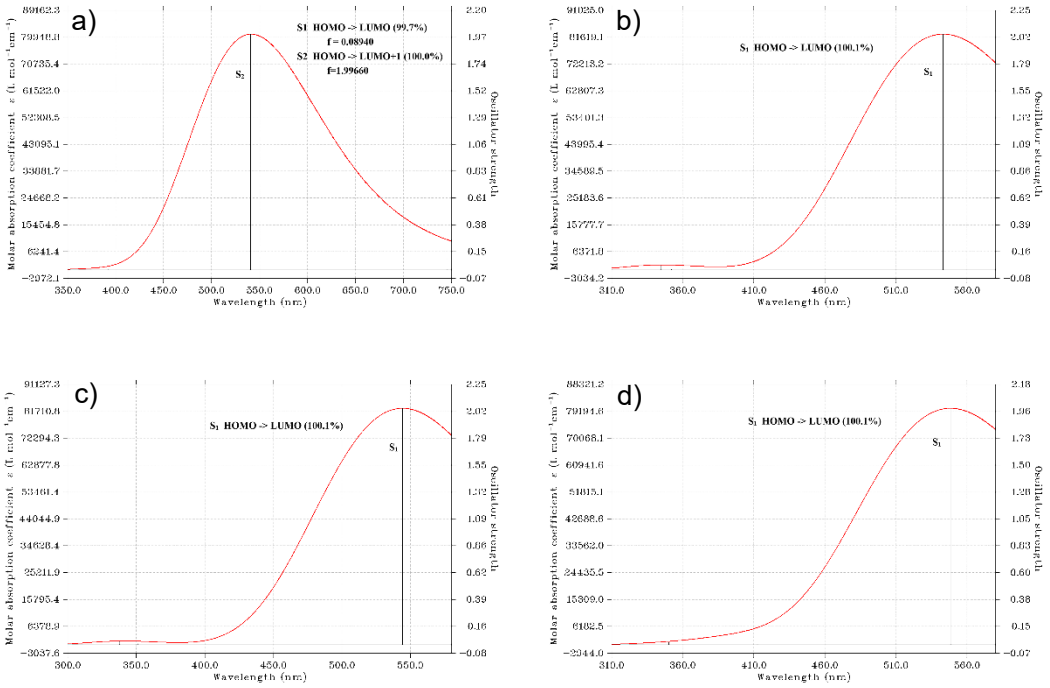

Fig. S7. Calculated absorption spectra with oscillator strengths and main orbital contributions of a) **Cy5-ph-NO$_2$,** b) **Cy5-ph-Cl,** c) **Cy5-ph-H,** d) **Cy5-ph-MeO**.

UV/vis titration and Fluorescence titration experiments

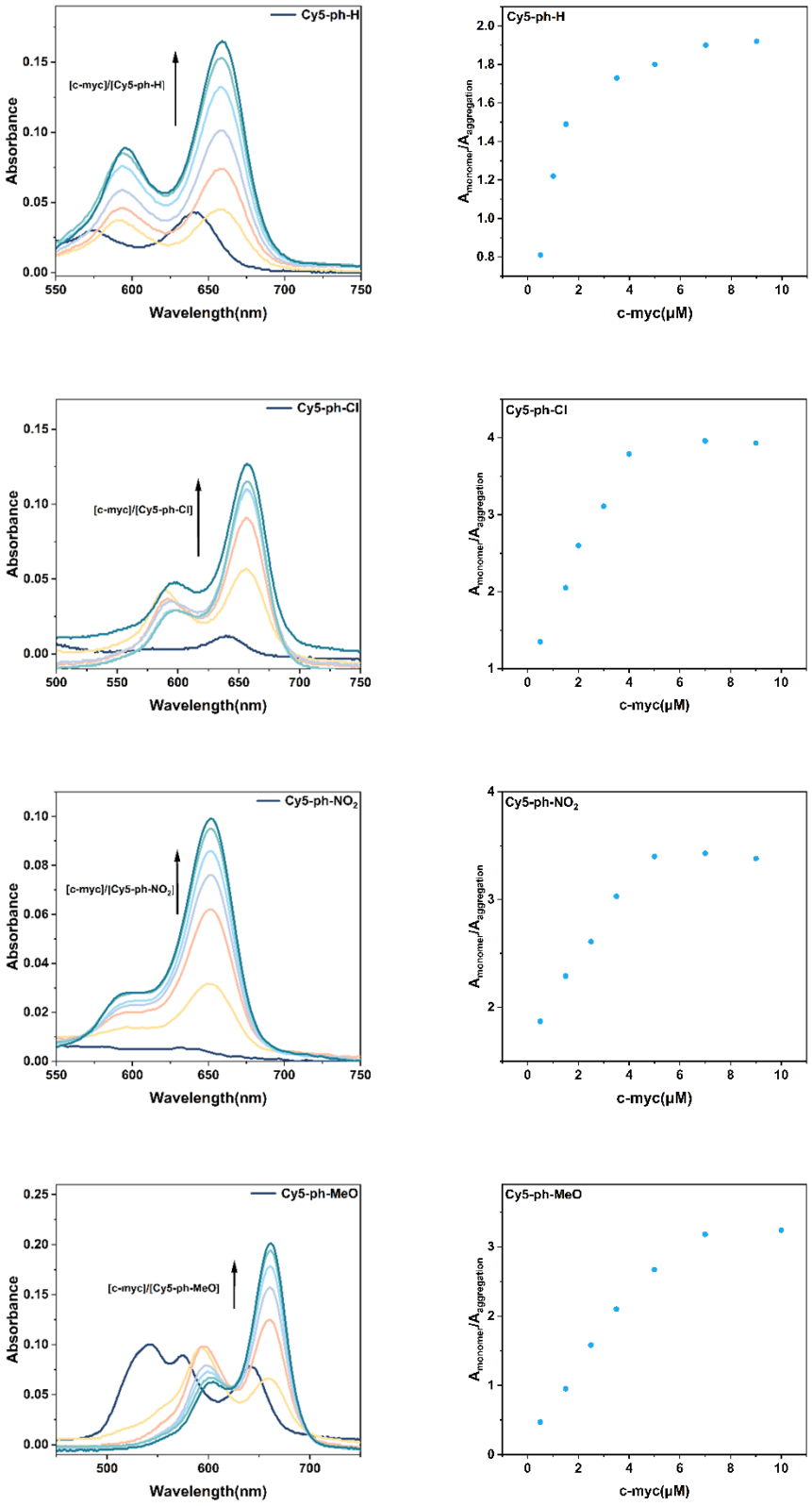

Fig. S8. UV/vis titration curves of 5 μM **Cy5-phs.**

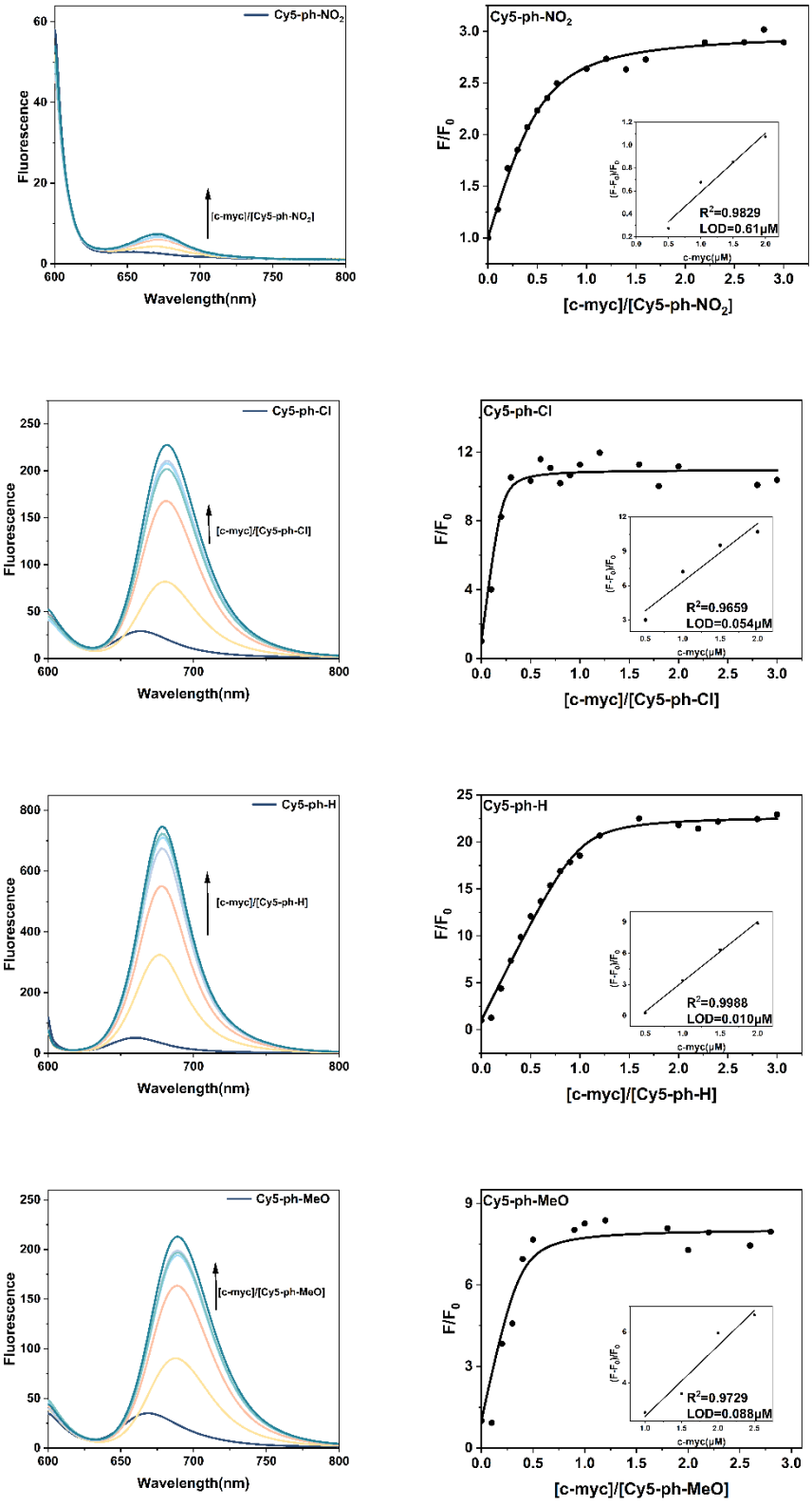

Fig. S9. Fluorescence titration curves of 5 μM **Cy5-phs.**

Table S5. The result of the dye binding to the G4 DNA

dye	G4	λ_{abs} (nm)	λ_{em} (nm)	F/F_0	K_a (10^6 M^{-1})	LOD (μm)	Φ
Cy5-ph-NO_2	c-myc	652	673	2.99	0.82	0.61	0.019
Cy5-ph-Cl	c-myc	657	682	10.97	3.27	0.054	0.39
Cy5-ph-MeO	c-myc	661	689	8.07	2.25	0.088	0.20
Cy5-ph-H	c-myc	659	679	22.81	6.30	0.010	0.65
	c-kit2	661	675	3.87	1.14	0.077	0.055
	htg22	661	675	2.21	0.95	0.14	0.15
	oxy28	659	674	3.42	0.059	0.29	0.13

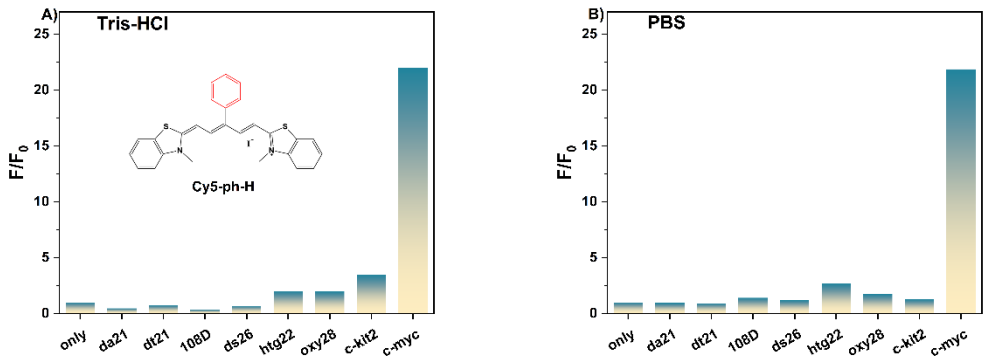

Fig S10. Histogram of fluorescence doubling effect after **Cy5-ph-H** (5 μM) binding to different DNA in **A)** Tris-HCl buffer (60 mM K^+) and **B)** PBS buffer (60 mM K^+).

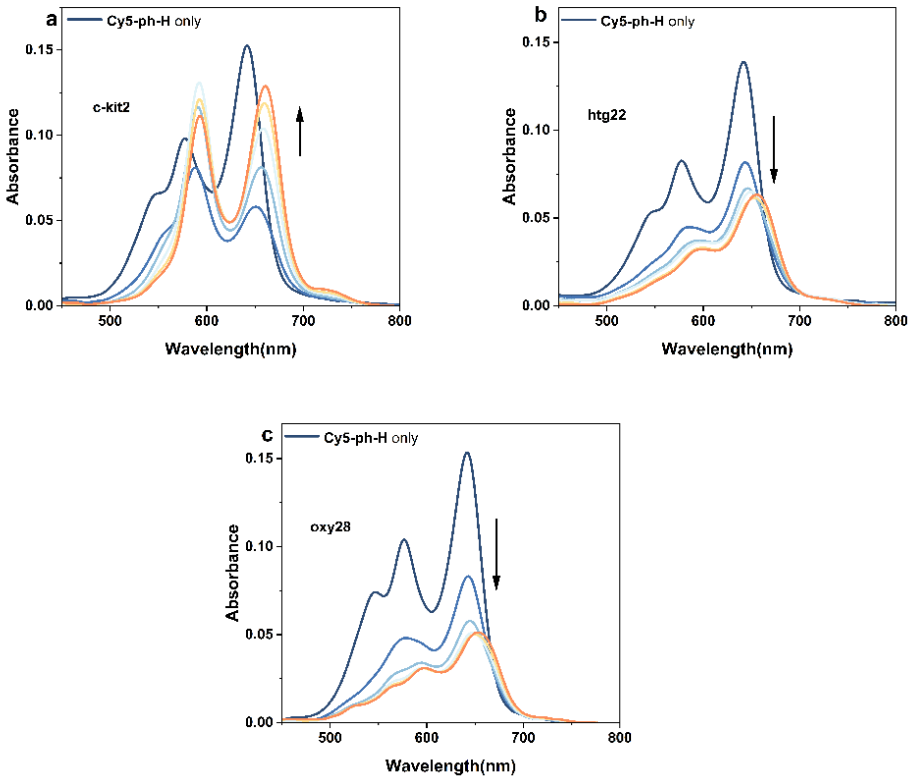

Fig. S11. UV/vis titration curves of **Cy5-ph** (5 μM) with stepwise addition of G4-DNAs ((a) c-kit2, (b) htg22, and (c) oxy28) in 10 mM Tris-HCl buffer, 60 mM KCl, pH 7.4

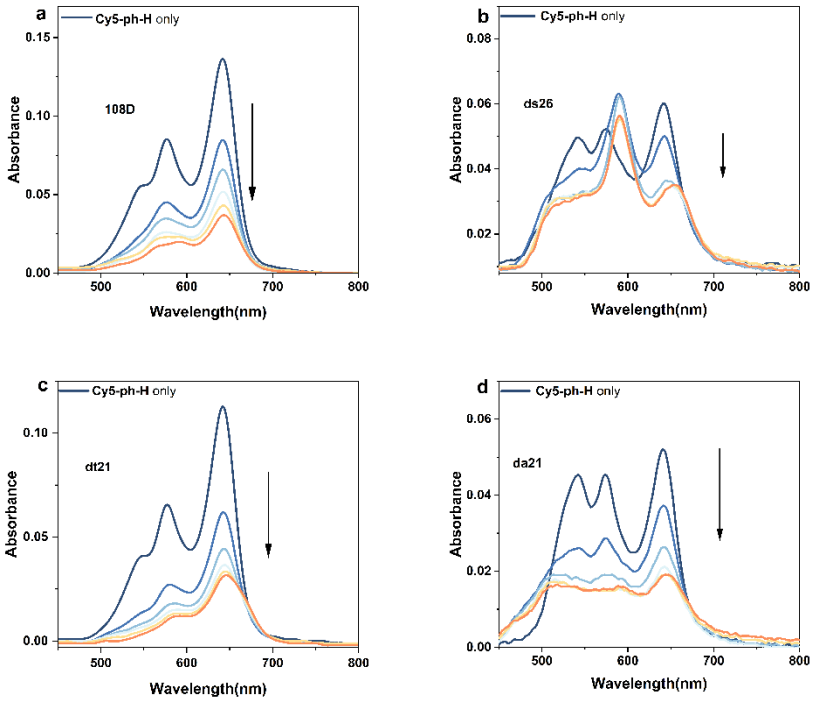

Fig. S12. UV/vis spectroscopic titration of **Cy5-ph** (5 μM) with stepwise addition of dsDNA ((a) 108D, (b) ds26) and ssDNA ((c) dt21, (d) da21) in 10 mM Tris-HCl buffer, 60 mM KCl, pH 7.4.

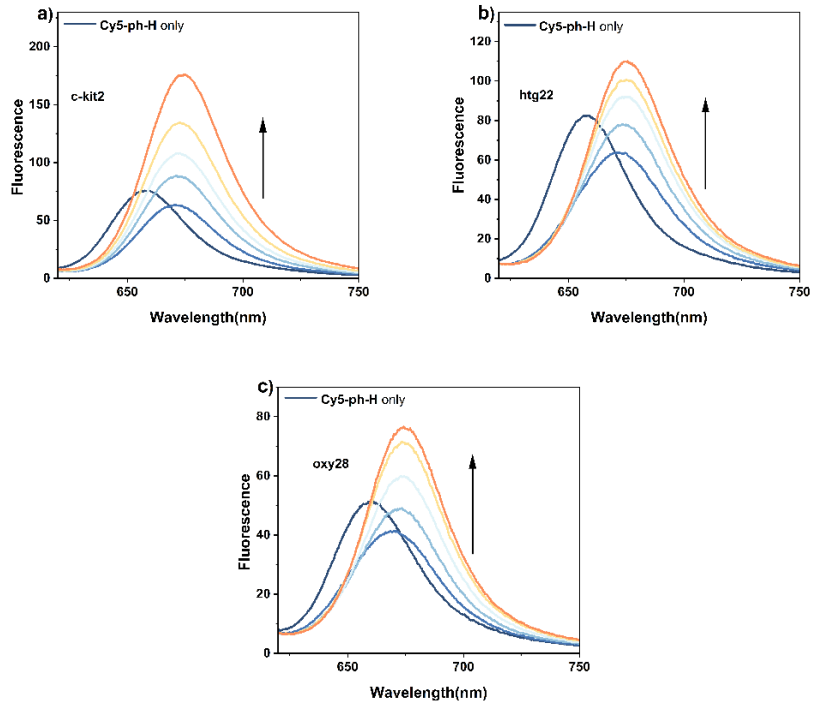

Fig. S13. Fluorescence titration curves of **Cy5-ph-H** (5 μM) with stepwise addition of G-DNAs ((a) c-kit2, (b) htg22, and (c) oxy28) in 10 mM Tris-HCl buffer, 60 mM KCl, pH 7.4

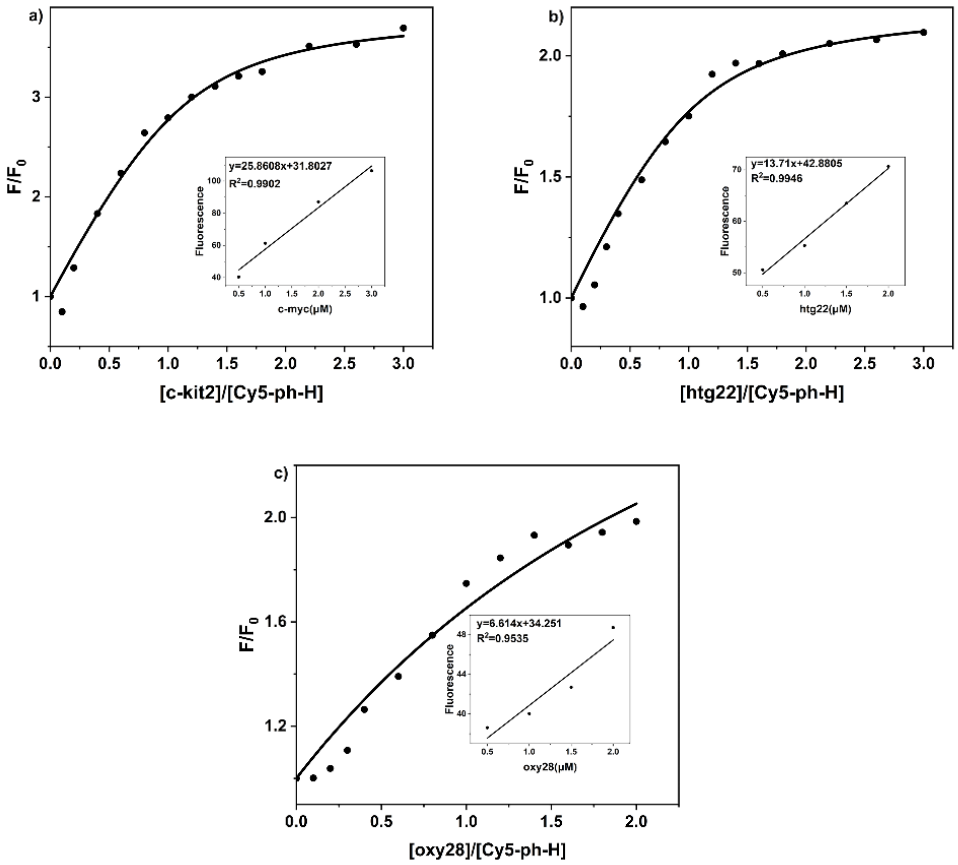

Fig. S14. Fitting plot of emission intensity ratio at maximum emission wavelength of **Cy5-ph-H** titrated with G4s ((a) c-kit2: λ_{em}= 675 nm; (b) htg22: λ_{em}= 675 nm; (c) oxy28: λ_{em}= 674 nm; F_0: the fluorescence intensity of dye in the absence of G-DNA; F: the fluorescence intensity of dye in the present of G-DNA).

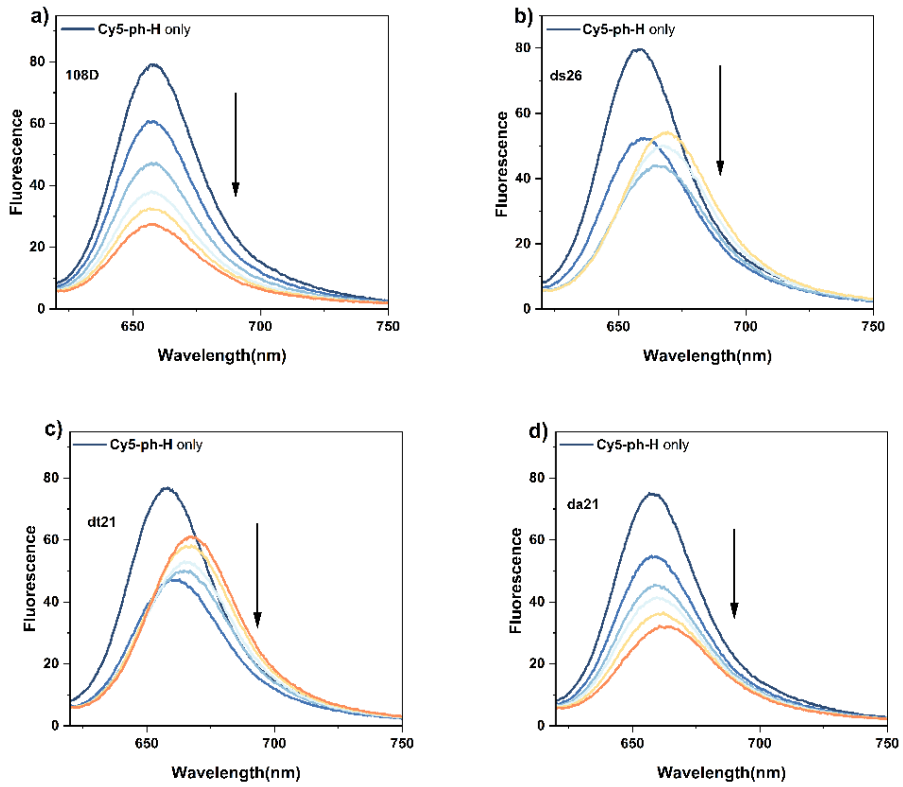

Fig. S15. Fluorescence spectroscopic titration of **Cy5-ph-H** with stepwise addition of dsDNA ((a) 108D, (b) ds26) and ssDNA ((c) dt21, (d) da21) in 10 mM Tris-HCl buffer, 60 mM KCl, pH 7.4. (arrows: 0-1.5 equivalents).

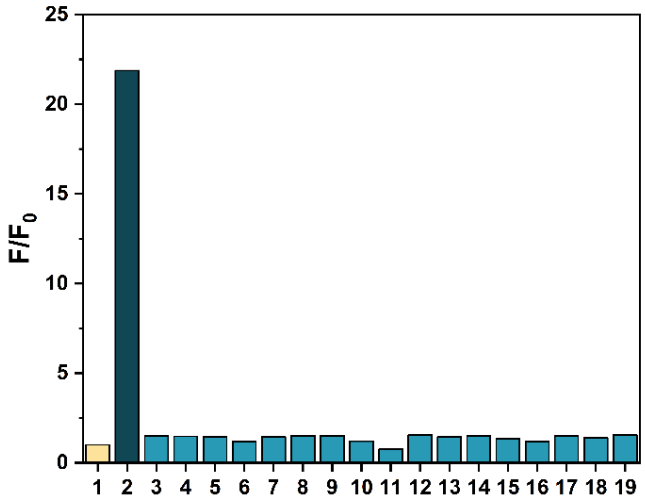

Fig S16. The fluorescence intensity of **Cy5-ph-H** (5 μM) towards other analytes (1: blank; 2: c-myc; 3: Ba^{2+}; 4: Ca^{2+}; 5: Cd^{2+}; 6: Cu^{2+}; 7: Fe^{3+}; 8: K^{+}; 9: Mg^{2+}; 10: Na^{+}; 11: Ni^{+}; 12: Pd^{2+}; 13: Cr^{3+}; 14: CO_3^{2-}; 15: NO_3^{-}; 16: SO_4^{2-}; 17 H_2O_2; 18: GSH; 19: Cys). λ_{ex} = 588 nm.

Job's plot

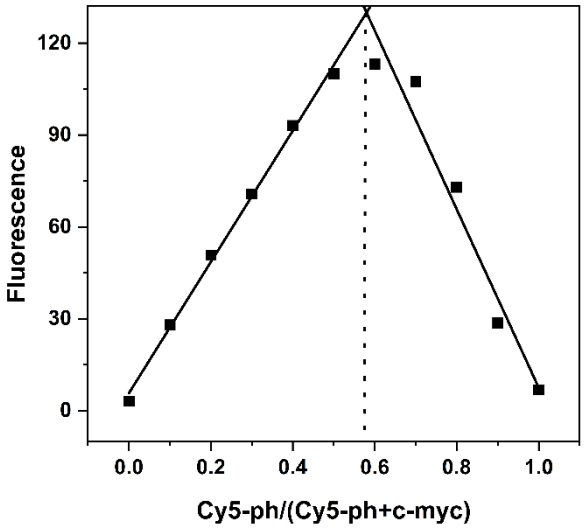

Fig. S17. The Job's plot analysis for the binding stoichiometry of **Cy5-ph-H** to c-myc.

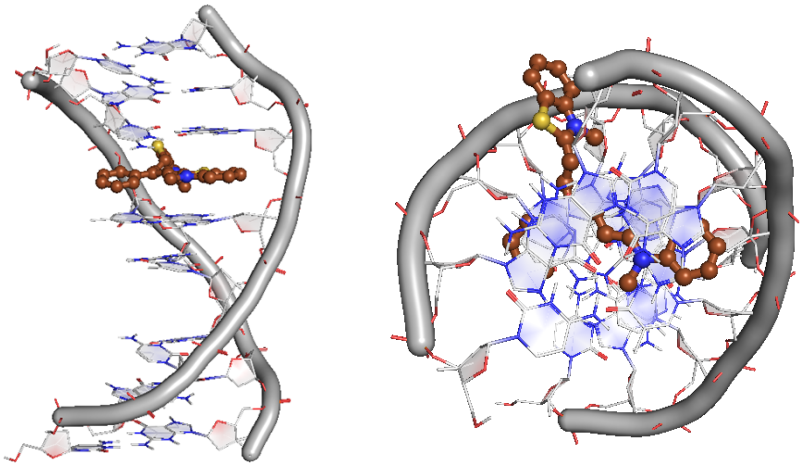

Fig S18. Molecular docking results of **Cy5-ph-H** and 108D: side view (left) and top view (right).

Circular Dichroism (CD)

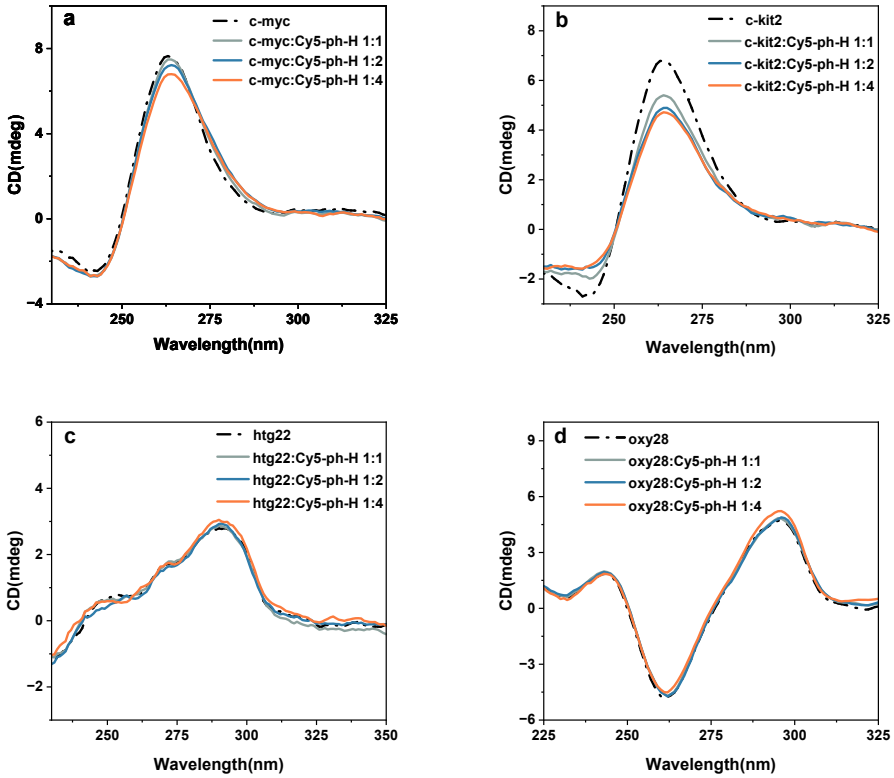

Fig. S19. CD spectra of 5 μM G4s ((a) c-myc, (b) c-kit2, (c) htg22 and (d) oxy28 with and without **Cy5-ph-H** in Tris-HCl buffer, 60 mM KCl, pH 7.4.

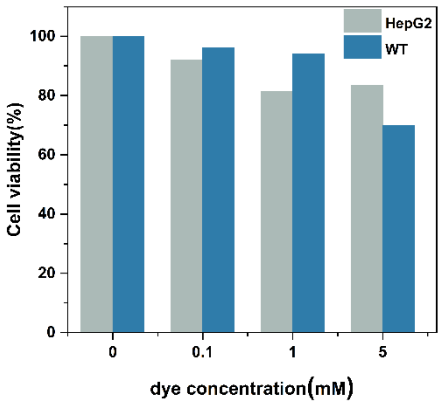

Fig. S20. Cells survival viability of HepG2 and WT were cultured with different concentrations of **Cy5-ph-H**.

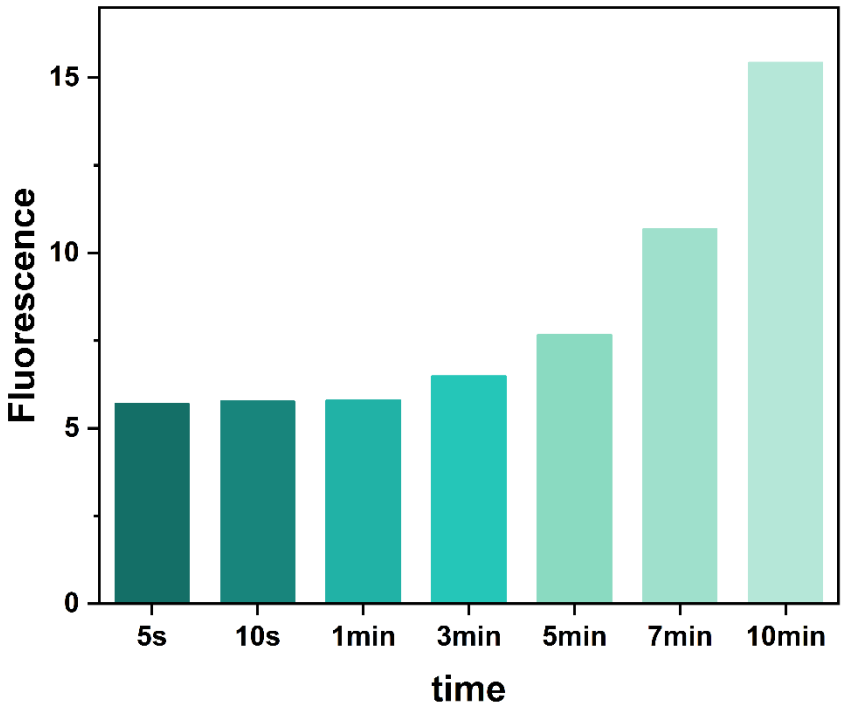

Fig S21. Average fluorescence intensity of time-progressive images at different time points after the addition of **Cy5-ph-H** (0.5 μM) from 5 s to 10 min.

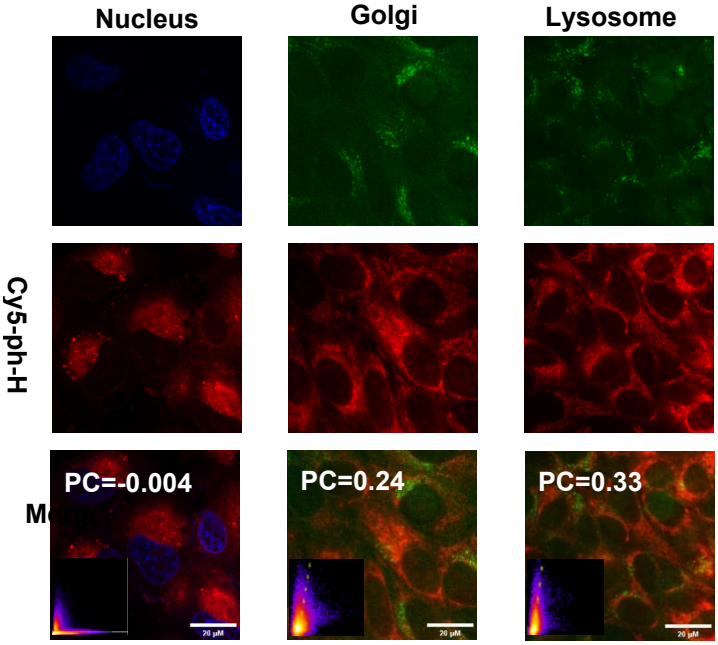

Fig S22. Co-localization confocal fluorescence imaging of live HepG2 cells were treated with 0.5 μM **Cy5-ph-H** (0.1% DMSO) then incubated with Hoechst 33342 (2 μg/mL) for 10min, Golgi green (5 μM) and Lyso-Tracker Green (0.075 μM), respectively. Scale bar: 20 μM.

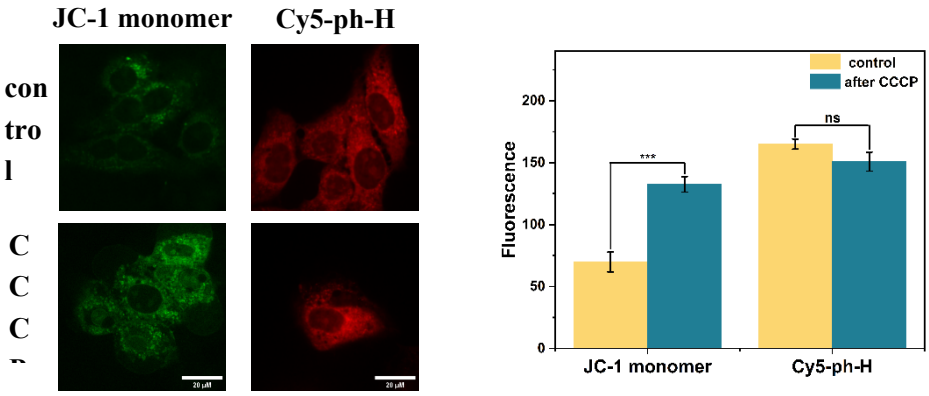

Fig S23. Confocal fluorescence microscope images of HepG2 cells incubated with JC-1 staining working solution (C2006, Beyotime Biotechnology) or 0.5 μM **Cy5-ph-H,** before and after the addition of 10 μM CCCP, respectively. The excitation wavelengths were 488 nm for JC-1 monomer and 640 nm for **Cy5-ph-H**. Scale bar: 20 μM.

Ⅲ ^{1}H NMR, ^{13}C NMR and HRMS

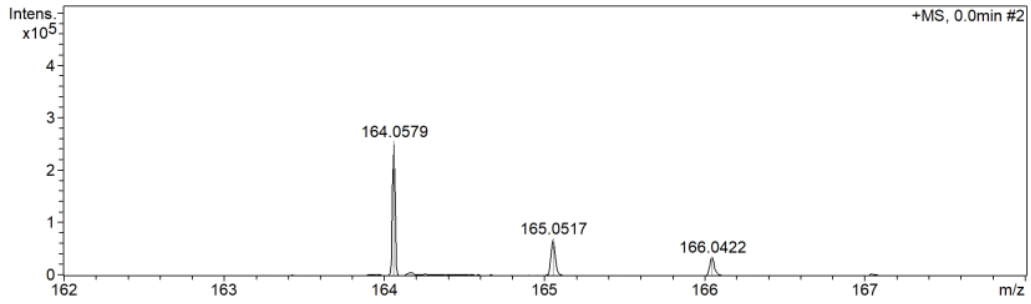

Figure S24. HRMS (ESI-TOF) spectrum of **1** (in CH_3OH).

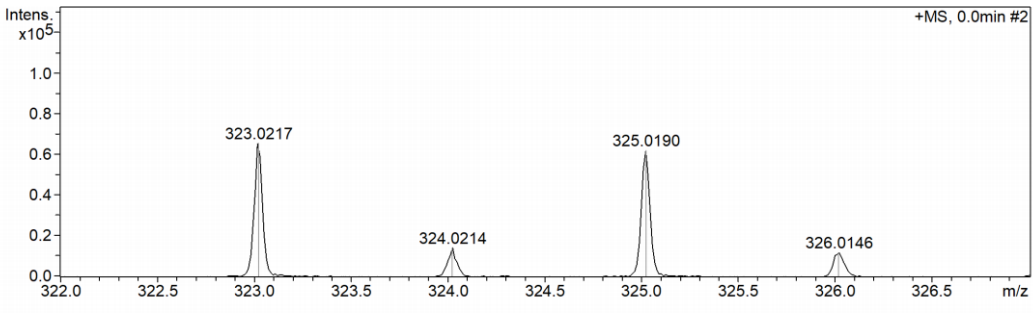

Fig. S25. HRMS (ESI-TOF) spectrum of **2** (in CH_3OH).

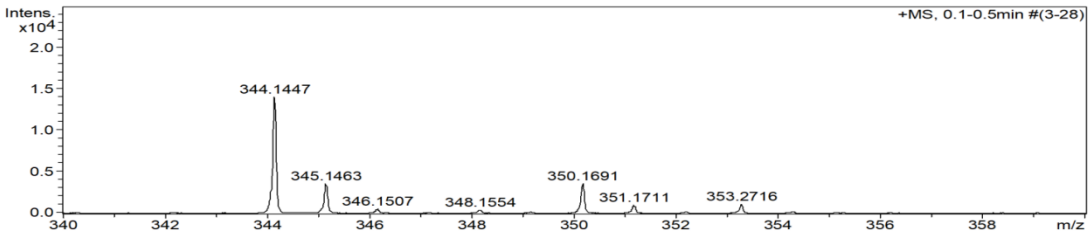

Fig. S26. HRMS (ESI-TOF) spectrum of **3a** in CH_3OH

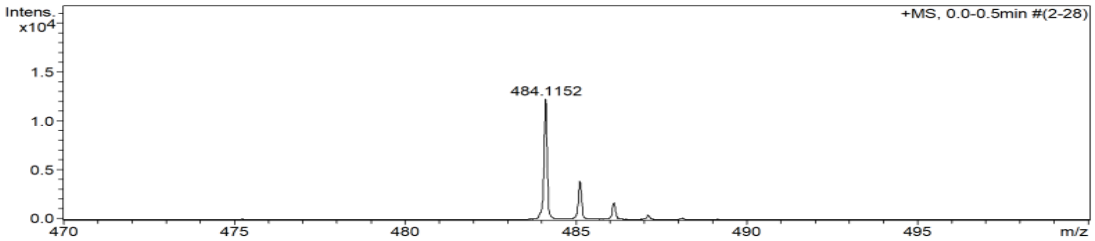

Fig. S27. HRMS (ESI-TOF) spectrum of **Cy5-ph-NO_2** in CH_3OH

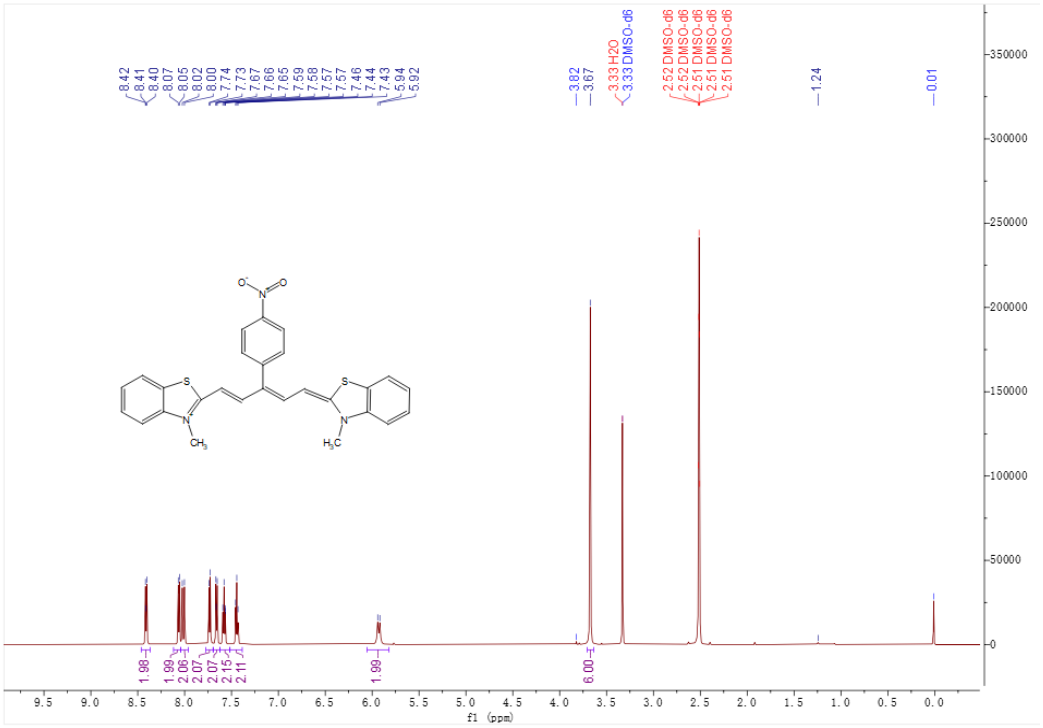

Fig. S28. [1]H NMR spectrum of **Cy5-ph-NO$_2$** in DMSO-d_6

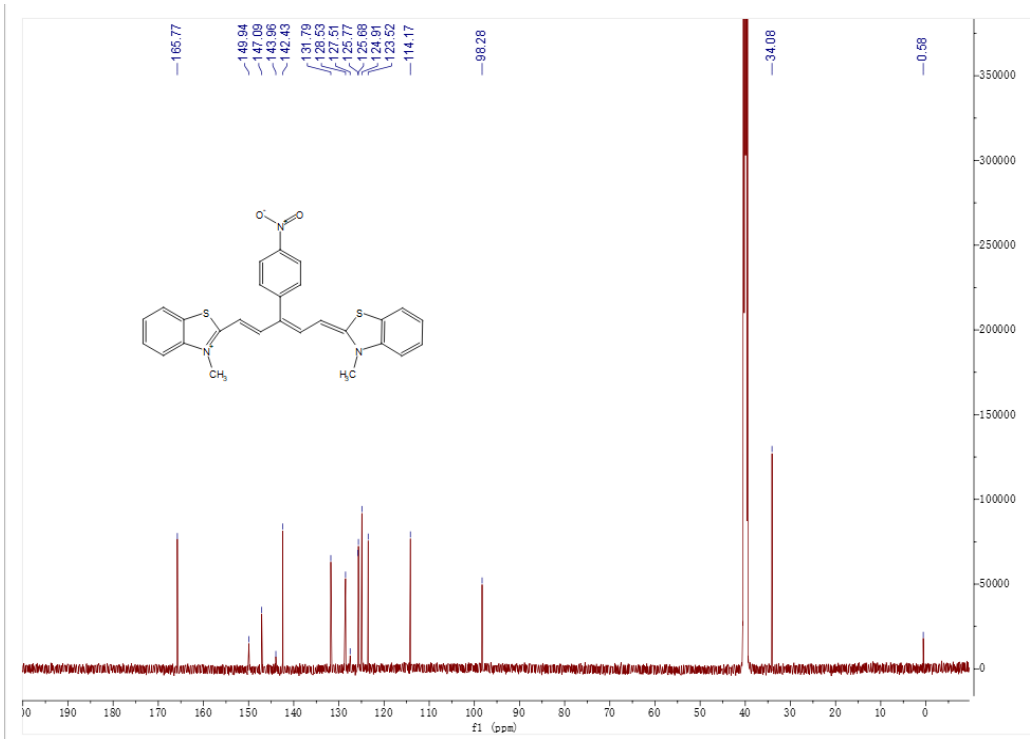

Fig. S29. [13]CNMR spectrum of **Cy5-ph-NO$_2$** in DMSO-d_6

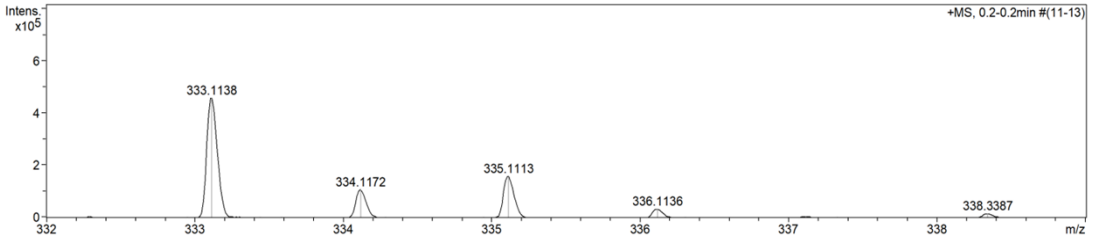

Fig. S30. HRMS (ESI-TOF) spectrum of **3b** in CH_3OH

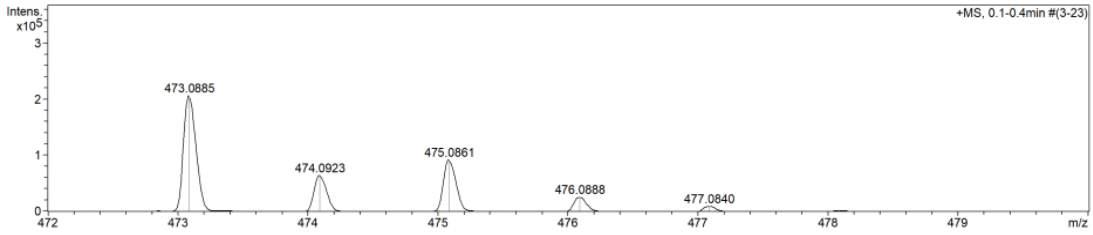

Fig. S31. HRMS (ESI-TOF) spectrum of **Cy5-ph-Cl** in CH_3OH

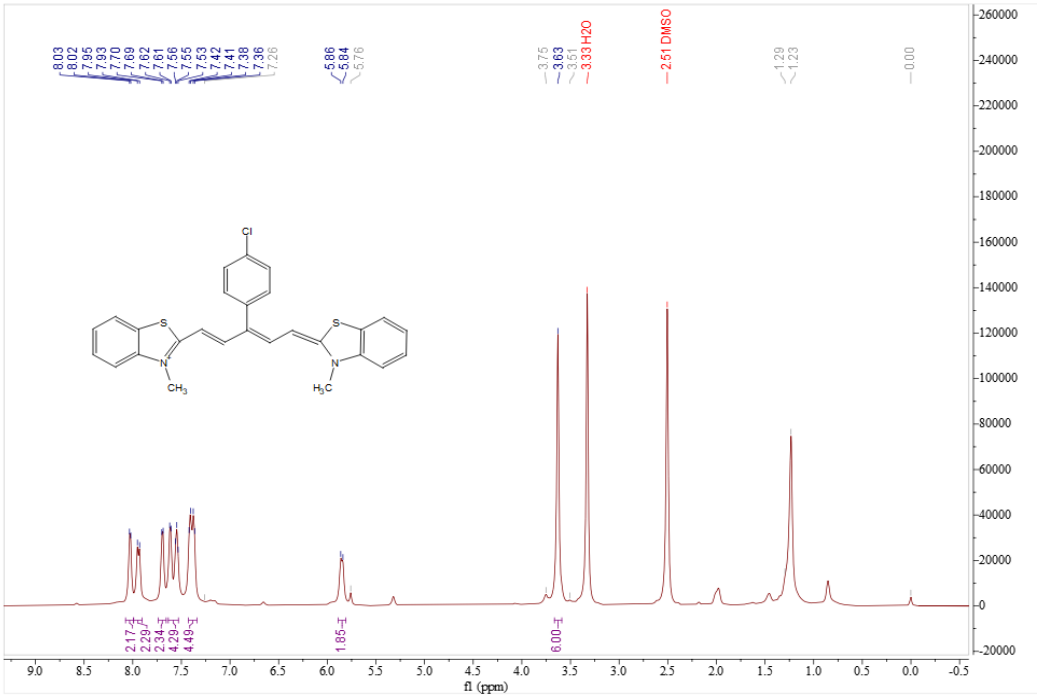

Fig. S32. ^{1}H NMR spectrum of **Cy5-ph-Cl** in DMSO-d_6

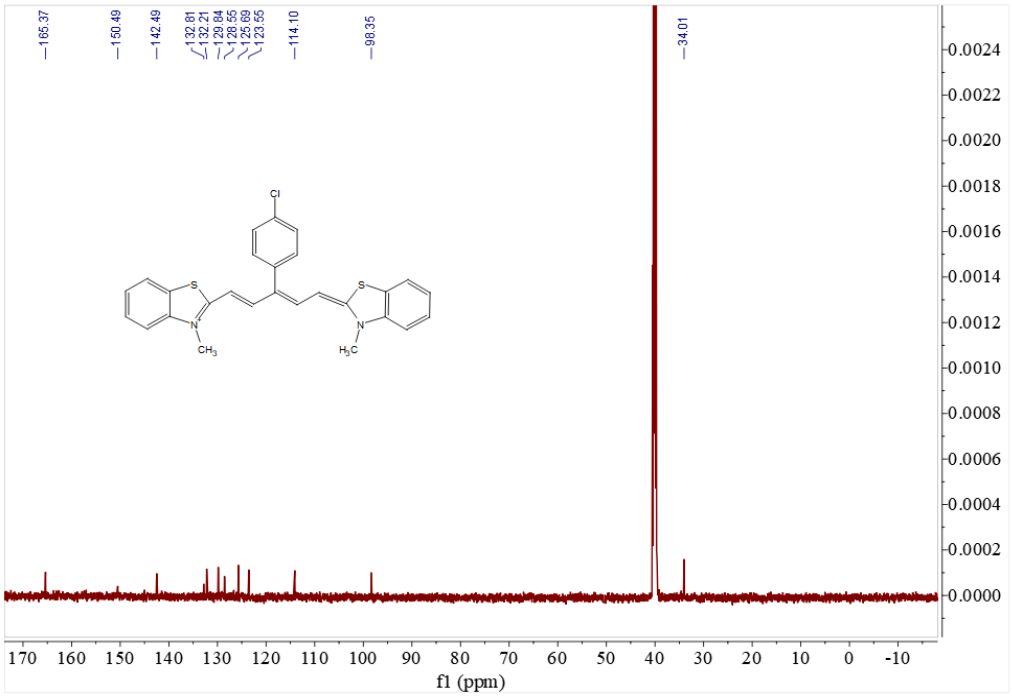

Fig. S33. ^{13}C NMR spectrum of **Cy5-ph-Cl** in DMSO-d_6

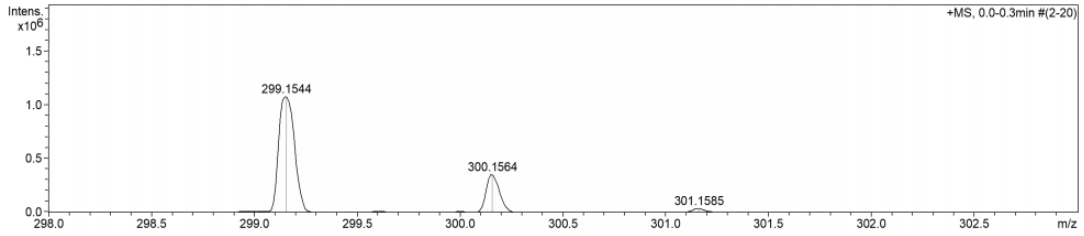

Fig. S34. HRMS (ESI-TOF) spectrum of **3c** in CH_3OH

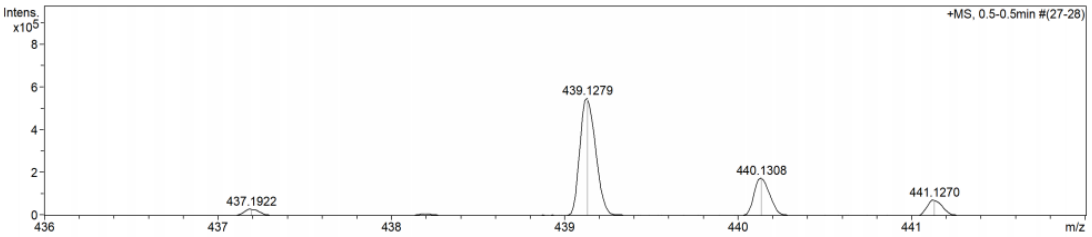

Fig. S35. HRMS (ESI-TOF) spectrum of **Cy5-ph-H** in CH_3OH

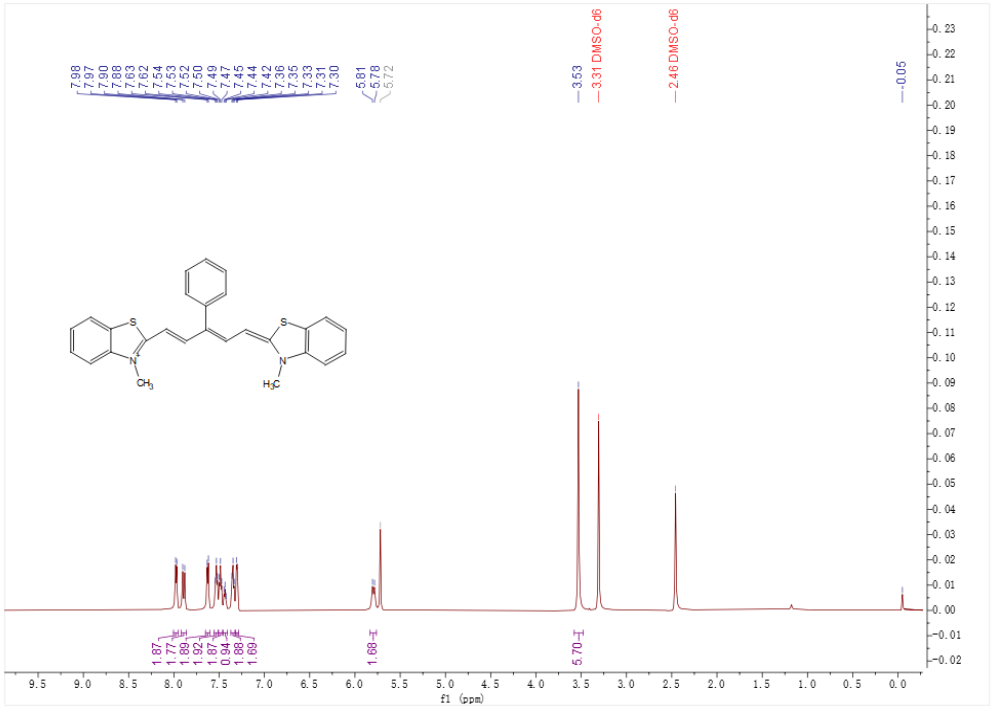

Fig. S36. [1]H NMR spectrum of **Cy5-ph-H** in DMSO-d_6

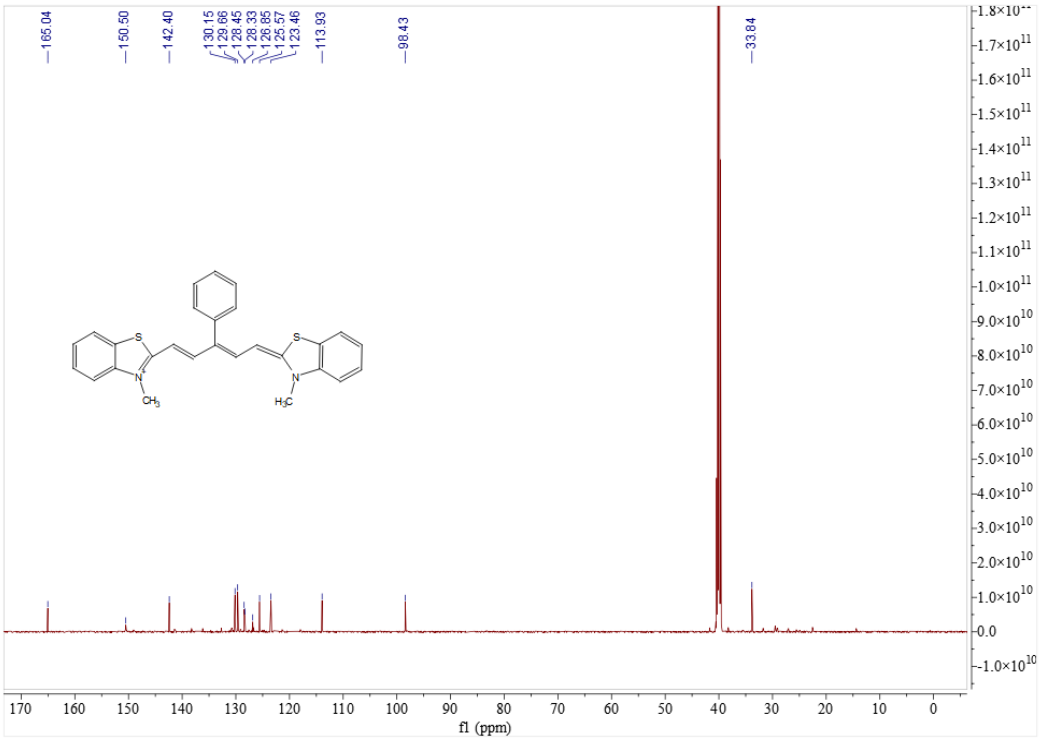

Fig. S37. [13]CNMR spectrum of **Cy5-ph-H** in DMSO-d_6

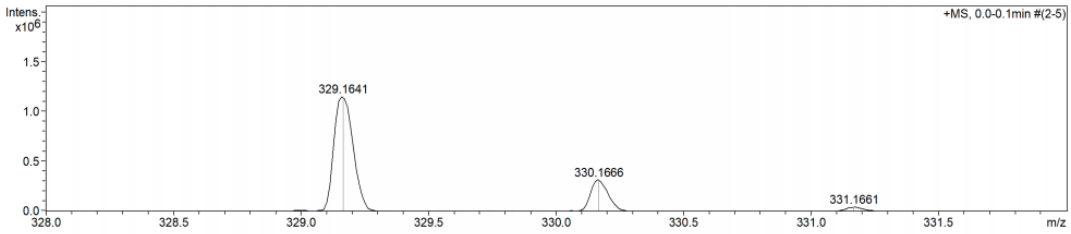

Fig. S38. HRMS (ESI-TOF) spectrum of **3d** in CH_3OH

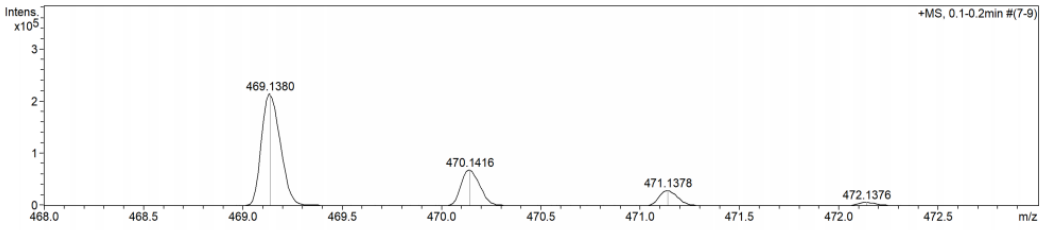

Fig. S39. HRMS (ESI-TOF) spectrum of **Cy5-ph-MeO** in CH_3OH

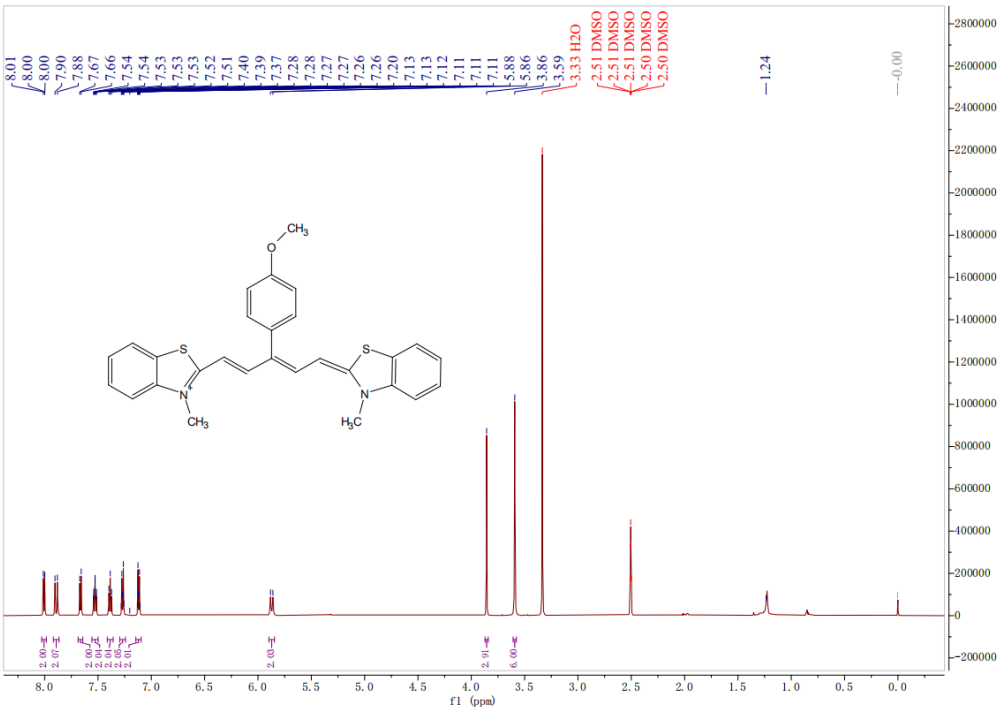

Fig. S40. ^{1}HNMR spectrum of **Cy5-ph-MeO** in DMSO-d_6

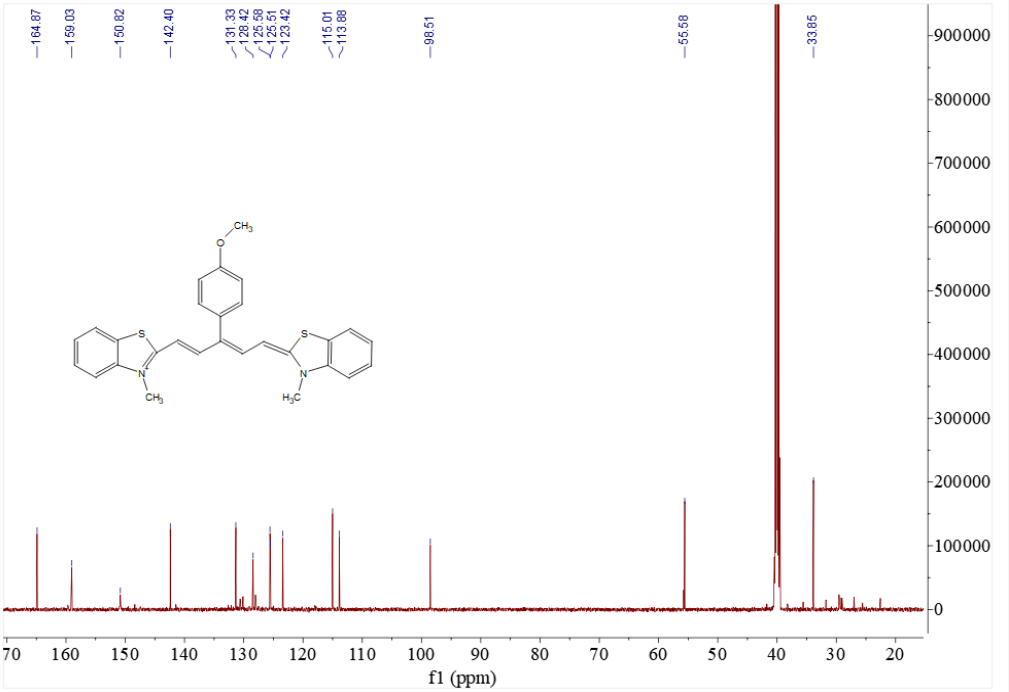

Fig. S41. ^{13}CNMR spectrum of **Cy5-ph-MeO** in DMSO-d_6

Ⅳ References

1 Y. Ji, Y. Wang, N. Zhang, S. Xu, L. Zhang, Q. Wang, Q. Zhang and H.-Y. Hu, *The Journal of Organic Chemistry*, 2018, **84**, 1299–1309.

2 G. Feng, X. Luo, X. Lu, S. Xie, L. Deng, W. Kang, F. He, J. Zhang, C. Lei, B. Lin, Y. Huang, Z. Nie and S. Yao, *Angewandte Chemie International Edition*, 2019, **58**, 6590-6594.

3 A. Alessi, M. Salvalaggio and G. Ruzzon, *Journal of Luminescence*, 2013, **134**, 385-389.

4 Gaussian 16, Revision C.01, M. J. Frisch, G. W. Trucks, H. B. Schlegel, G. E. Scuseria, M. A. Robb, J. R. Cheeseman, G. Scalmani, V. Barone, G. A. Petersson, H. Nakatsuji, X. Li, M. Caricato, A. V. Marenich, J. Bloino, B. G. Janesko, R. Gomperts, B. Mennucci, H. P. Hratchian, J. V. Ortiz, A. F. Izmaylov, J. L. Sonnenberg, D. Williams-Young, F. Ding, F. Lipparini, F. Egidi, J. Goings, B. Peng, A. Petrone, T. Henderson, D. Ranasinghe, V. G. Zakrzewski, J. Gao, N. Rega, G. Zheng, W. Liang, M. Hada, M. Ehara, K. Toyota, R. Fukuda, J. Hasegawa, M. Ishida, T. Nakajima, Y. Honda, O. Kitao, H. Nakai, T. Vreven, K. Throssell, J. A. Montgomery, Jr., J. E. Peralta, F. Ogliaro, M. J. Bearpark, J. J. Heyd, E. N. Brothers, K. N. Kudin, V. N. Staroverov, T. A. Keith, R. Kobayashi, J. Normand, K. Raghavachari, A. P. Rendell, J. C. Burant, S. S. Iyengar, J. Tomasi, M. Cossi, J. M. Millam, M. Klene, C. Adamo, R. Cammi, J. W. Ochterski, R. L. Martin, K. Morokuma, O. Farkas, J. B. Foresman, and D. J. Fox, Gaussian, Inc., Wallingford CT, 2016.

5 T. Lu and F. Chen, *Journal of Computational Chemistry*, 2012, **33**, 580-592.